KAMILLA EMILY SANTOS SILVA

Topology Optimization Methods For Tower Structural Designs Involving Fluid-structure Interaction and Soil-Structure Interaction

Revised version

São Paulo

2023

KAMILLA EMILY SANTOS SILVA

Topology Optimization Methods For Tower Structural Designs Involving Fluid-structure Interaction and Soil-Structure Interaction

Revised version

São Paulo

2023

Este exemplar foi revisado e corrigido em relação à versão original, sob responsabilidade única do autor e com a anuência de seu orientador.

São Paulo, __24__ de _____abril_____ de ___2023___

Assinatura do autor: _____Kamilla E. S. Silva_____

Assinatura do orientador: _____Renato Picelli Sanches_____

Catalogação-na-publicação

Dedicatória

A minha amada mãe, Geneci.

Agradecimentos

A minha familia, por todo incentivo e apoio em toda minha tragetória.

Ao meu orientador Renato Picelli, pelo imenso conhecimento compartilhado com a máxima dedicação e humildade. Por sua compreensão, amizade e confiança a qual tornou possivel esse trabalho. Uma grande referência de profissional e amigo o qual levarei para sempre.

Ao professor Gil Ho Yoon, por todo o suporte, atenção e conhecimento agregado a essa jornada.

Ao meu primeiro orientador, René Quispe, pelo grande apoio e incentivo na escolha da minha trajetória.

Aos meus amigos, pelo apoio e momentos de descontração vividos.

Acknowledgements

Resumo

SILVA, K. E. S. **Métodos de Otimização Topológica para Projetos de Torres Estruturais Envolvendo Interação Fluido-Estrutura e Interação Solo-Estrutura**. 2023. Dissertação (Mestrado). Escola Politécnica da Universidade de São Paulo, São Paulo, Brasil.

Esse trabalho visa desenvolver e aplicar metodologias de otimização topológica para projetos otimizados de estruturas tipo torre envolvendo duas importantes classes de problemas Multifísicos: a Interação Fluido-Estrutura (FSI, na sigla em inglês) e a Interação Solo-Estrutura (SSI, na sigla em inglês). A análise e modelagem de problemas envolvendo mais de um fenômeno físico é um tópico potencialmente desafiador no contexto de Otimização Topológica (OT). O forte acoplamento entre os domínios físicos que, em alguns casos, acarreta a mudança constante das cargas estruturais em termos de localização, direção e magnitude ou a presença de mais de um tipo de material no mesmo domínio são desafios presentes neste tipo de problema. Neste trabalho, duas metodologias baseadas em um método binário são desenvolvidas para projetar estruturas com limites bem definidos e mitigar as principais dificuldades encontradas na otimização topológica aplicada a sistemas multifísicos. O método de Otimização Topológica de Estruturas Binárias (TOBS), o qual é baseado em programação linear inteira e emprega variáveis binárias $\{0,1\}$, é usado como formulação base para encontrar os desenhos fluido-estrutura e solo-estrutura otimizados. Na classe de problemas FSI, exemplos numéricos 3D são resolvidos e grandes deslocamentos são incluídos. Nos sistemas SSI, cargas estáticas e dinâmicas são consideradas. Pelo melhor do conhecimento do autor, este é o primeiro trabalho a empregar otimização topológica binária no projeto FSI incluindo grandes deslocamentos e variáveis estritamente binárias no projeto de sistemas SSI. Problemas numéricos são resolvidos e as vantagens de cada metodologia são particularmente apontadas em cada capítulo.

Palavras-chave: Otimização topológica, Estruturas tipo torre, Variáveis de projeto binárias, Interação Fluido-estrutura, Interação Solo-estrutura.

Abstract

SILVA, K. E. S. **Topology Optimization Methods For Tower Structural Designs Involving Fluid-structure Interaction and Soil-Structure Interaction**. 2023. Thesis (Masters). Polytechnic School of the University of São Paulo, São Paulo, Brazil.

This work aims to develop and apply topology optimization methodologies for optimized designs of tower-like structures involving two important classes of Multiphysics problems: Fluid-Structure Interaction (FSI) and Soil-Structure Interaction (SSI). The analysis and modeling of problems involving more than one physical phenomenon is a potentially challenging topic in the topology optimization (TO) framework. The strong coupling between the physical domains which, in some cases, entails the constant change of structural loads in terms of location, direction and magnitude or the presence of more than one type of material in the same domain are challenges present in this type of problem. In this work, two methodologies based on a binary method are developed in order to design structures with well-defined boundaries and mitigate the main difficulties encountered in the application of topology optimization in multiphysics systems. The Topology Optimization of Binary Structures (TOBS) method, which is based on integer linear programming and employs binary variables $\{0,1\}$, is used as the base formulation in order to find optimized fluid-structure and soil-structure layouts. In the FSI class of problems, 3D numerical examples are solved and large displacements are included. In the SSI systems, static and dynamic loads are considered. To the best of author's knowledge, this is the first work to employ binary topology optimization in FSI design including large displacements and strictly binary variables into the design of SSI systems. Numerical problems are solved and the the advantages of each methodology are particularly pointed out in each chapter.

Keywords: Topology Optimization, Tower-like structures, Binary design variables, Fluid-structure interaction, Soil-structure interaction.

List of Figures

Contents

1   INTRODUCTION

This work proposes and investigates structural topology optimization methodologies related to the design of structural towers considering two different types of multiphysics analyses: Fluid-Structure Interaction (FSI) and Soil-Structure Interaction (SSI). Applications can include win turbines, ocean and civil structures, among others. The first part of the thesis addresses the optimization of FSI problems including nonlinear structural responses. The second part presents the design optimization of foundations for structural towers subject to static and dynamic loads. For this, a binary methodology is employed in order to find the optimized designs for each class of problem. Thereby, the optimized structural solutions obtained are based on clear and defined boundaries, which is an advantage for multiphysics problems. Despite the distinction between the two multiphysics systems, the methodologies used in this work share several concepts and are based on the same optimization method. Thus, this chapter begins by exposing the motivation and the objectives of the presented work. Then, a brief explanation addressing the basic concepts of structural optimization and the list of publications generated from this work are presented. Ultimately, the chapter ends by briefly describing the structure of the work.

1.1   Motivation

In recent decades, the area of structural engineering has been faced with structures of increasing complexity. The increase in design requirements related to economic and environmental issues has increasingly required the advancement of technologies in order to obtain high performance designs in terms of functionality and efficiency. An example of this scenario is wind turbine structures. The growing interest in renewable energies since the first oil crisis of the 1970s has spurred the development of alternative technologies in order to decrease greenhouse gas emissions and its effect on the global warming [3]. Since then, energy production through wind turbines has grown exponentially around the world being the renewable energy source with the fastest growth among all other available renewable sources [4]. As a consequence, technologies applied to wind turbines have also followed the same path. However, the structural design of wind energy capture and generation systems still face major challenges in terms of analysis and modeling.

The complexity of wind turbine designs is mostly due to the interaction between different physical phenomena and the effects arising from them, as illustrated in Fig. 1. Such structures are mainly loaded by dynamic loads derived from wind currents and waves which generate viscous and inertial effects on the structure – a scenario difficult to reconcile [5, 6]. Furthermore, uncertainty about soil behavior is also a notable challenge that is often neglected in the literature. This interaction is generally observed as dynamic effects on the turbine [7]. As a result of the mentioned loading elements, wind turbines are prone to fatigue damage, vibration issues and nonlinear structural responses – fundamental factors to be considered [7, 8]. In addition to the ineffectiveness of the design, the neglect of such factors can lead to catastrophic structural damage, e.g. breaking the rotor blades or cracks in the foundation structure, as shown in Fig. 2 [9, 1, 2]. In such context, taking into account the high complexity and non-intuitiveness designs of these systems, optimization methods emerge as a fundamental tool to design structures with
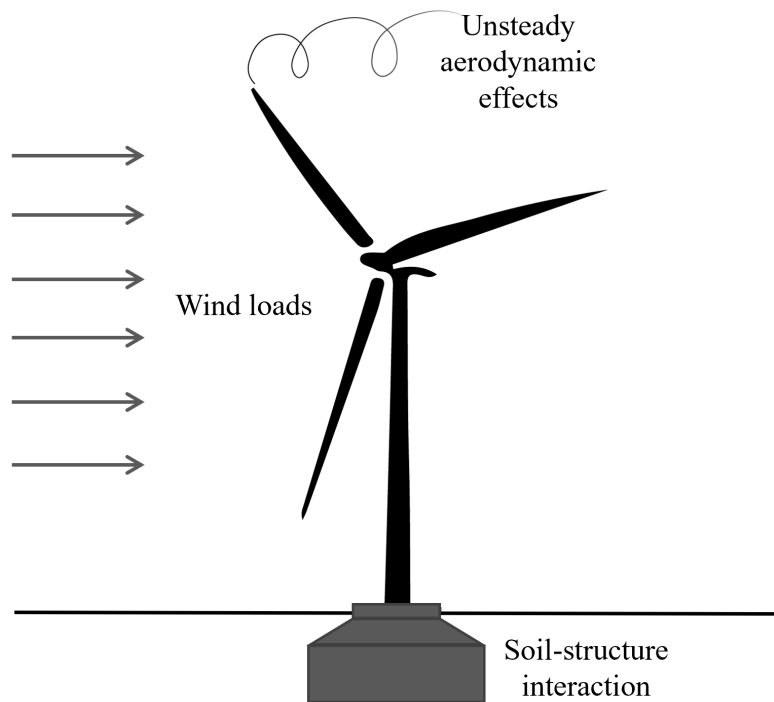
Figure 1: Loads conditions and challenging phenomena in a wind turbine.

higher performance in terms of safety, innovation and efficiency.

As a powerful design tool, Topology Optimization (TO) methods have gained prominence in the engineering area due to its great potential to provide efficient designs freely, from full initial domains without the need for an initial solution. The central idea of the method consists of the best distribution of material within a predetermined domain considering an objective function and prescribed design criteria [10]. TO methods stands out among other optimization methods – such as parametric or shape – due to their high flexibility and applicability since the material is freely distributed within the design domain, which allows the creation of new structural contours or the removal of the initial ones. TO is largely applied to the automotive and aerospace industry, but slightly focused on the design of tower-like structures such as wind turbines [7, 11]. Therefore, we are far from making the most we can from Topology Optimization for Multiphysics problems in general, and the development of new methodologies in order to push the limits of this design tool is necessary.

The reasons that explain this underexplored scenario in terms of optimization topic are various, but the complex characteristics regarding this sort of mechanical system – harsh environment and complex mechanical modeling – are certainly a bottleneck for researchers. A large part of the loads acting on these structures can be studied via Fluid-Structure Interaction (FSI). FSI systems are known for their strong coupling, i.e., the fluid loads acting on the structure strictly depend on the structural boundary [12, 13]. The modeling and analysis challenges are due to the possibility of changing the loading throughout the optimization in terms of location, direction and magnitude [14, 15]. In such cases, clear tracking of the fluid-structure interface along with the correct imposition of coupling conditions are crucial factors to be computed. Although there are many studies involving TO in FSI problems in the literature, most remain almost restricted to small deformations [16]. However, the inclusion

Figure 2: Examples of structural damage in wind turbine systems due to structural design failure: (a) structural tower collapse (Shreve, 2018) [1] and (b) collapsed structure due to cracks in the foundation (Fowler, 2021) [2].

of nonlinear geometric analysis allows solutions closer to a realistic design since the structure may undergo large displacements during the working period – i.e., the energy production – and not only under extraordinary cases, e.g. in extreme weather conditions [5]. In addition to this scenario, the Soil-Structure Interaction (SSI) can also be mentioned. SSI is a phenomenon slightly addressed in the design optimization of structures. Nevertheless, the efficient design of geotechnical structures – such as the structural foundation – has a direct influence on the performance of the main structural system when it comes to macrostructures, structures sensitive to vibrations or subject to unstable working conditions. Large uncertainties about soil behavior, in addition to the different types of materials involved in the problem, are some of the reasons that explain the scarcity of studies in this area into the TO framework. The optimization of the structural topology in foundation structures can provide optimized layouts and designs with higher functionality to support the loads imposed on the structural system, in addition to the lower usage of material. Since the support structure (foundation and structural tower) has the highest cost share in wind turbines, the lower usage of material is a significant advantage in this sort of system [17]. Furthermore, accounting for the effects arising from the interrelation between the structural tower and the foundation is fundamental in the design of wind turbines since the structural response of the system is dominated by the connection of both elements [5].

In this context, in order to mitigate and overcome the challenges mentioned, this work aims to develop topology optimization methodologies for tower-like structures involving FSI and SSI systems. Two different methodologies are developed and applied separately to each class of multiphysics system, which are related to two main components of this sort of structural system: the tower and the structural foundation. Large displacements are considered for the FSI problems. Furthermore, in SSI systems, since the foundation structure is in direct contact with the soil, two different materials are considered in the design domain: soil and structural foundation material. From this, a larger design domain space is provided in addition to the optimization of both elements. Topology optimization methods have reached a high level of maturity which has allowed the solution of multiphysics problems in different types of systems. However, the classic TO frameworks are commonly addressed using methods based

on intermediate densities, e.g. the SIMP (Solid Isotropic Material with Penalization) method. Although these methods are classic in the topology optimization field and demonstrating great efficiency in most cases, the solutions obtained by such approaches present a lack of explicit structural boundaries resulting from the use of intermediate values. On the other hand, binary methods provides interesting solutions when applied to multiphysics problems. This class of methods holds the benefit of dealing with integer variables $\{0, 1\}$ which promotes a clear distinction between physical and domain boundaries, a significant advantage for multiphysics problems. The TOBS (Topology Optimization of Binary Structures) method [18] shows promise in the application of problems involving multiphysics problems [15, 19]. The method employs design binary variables $\{0,1\}$ – which avoids numerical problems arising from the adoption of intermediate densities – and it is based on integer linear programming. In this way, fully discrete optimized structures with clear physical boundaries are provided. Based on this, the TOBS method will be applied as a standard formulation for optimization of soil-structure and fluid-structure systems.

1.2 Objectives

The **aim** of this work is to develop topology optimization methodologies applied to tower-like structure systems. The TOBS method will be employed due to its ability to create clear structural boundaries and interfaces, in addition to its high potential in dealing with multiphysics problems.

The **objectives** are:

1. To develop topology optimization methodologies applied to tower-like structure designs considering FSI and SSI systems.

2. To develop and investigate a topology optimization methodology applied to FSI problems including large displacements.

3. To develop and investigate a topology optimization methodology for structural foundation designs considering static and dynamic loads.

1.3 Topology optimization

In a general concept, structural optimization consists of a set of numerical methods that aim to obtain designs with higher functionality according to an established objective, taking into account one or more constraints inherent to the design. For this, structural optimization methods seek the best structural configuration within a reference domain by modifying the parameters/state variables in order to improve the structure's performance. Structural optimization methods can be classified into three main classes: parametric optimization, shape optimization and topology optimization [10]. Figure 3 shows a representation of the three classes of optimization.

In parametric optimization, a structure is optimized from a known and predefined domain, which remains fixed throughout the optimization. In this way, only the geometric parameters (height, width, thickness, among others) are modified during the optimization in order to obtain
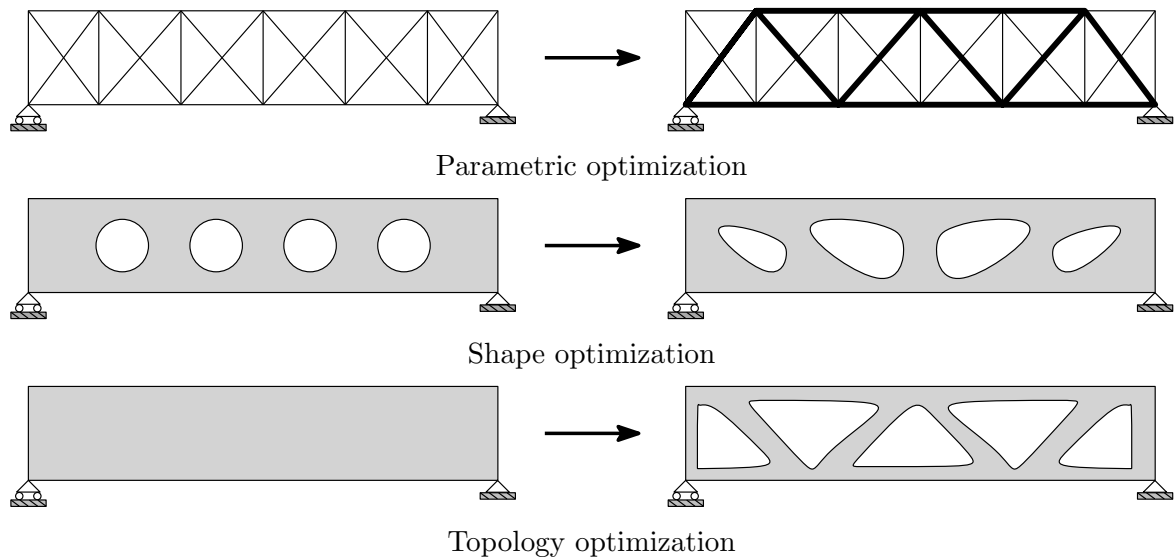
Figure 3: Main classes of structural optimization methods: parametric optimization, shape optimization and topology optimization.

a structure with better performance. Maximizing the structural stiffness by modifying the cross-sectional area of some structural member is an example of a problem achieved by parametric optimization.

In shape optimization, the topology of the structure remains fixed where only the structural contours (internal and external) can be modified. Since the structural topology is fixed, the optimization problem remains restricted to a specific number of design variables. Optimization takes place by changing structure connections – the nodal coordinates, for example, for portico or truss structures – or structural boundaries for continuous structures.

Topology optimization has as its central objective the best distribution of material within a pre-established design domain considering the design criteria imposed on the problem. Therefore, this class of methods can be approached as a combination or extension of the methods mentioned above. Known as a powerful design tool, topology optimization has greater flexibility compared to other optimization methods due to the possibility of obtaining high-performance designs, freely from full initial domains and without the need for an initial solution. Throughout the optimization process, the material can be freely distributed which allows the creation and/or change of structural contours.

Regardless of the class, optimization problems are composed of three main components which are briefly explained bellow.

- Design variables: The design variables refer to the problem variables/parameters which are manipulated in order to obtain the optimized structural configuration. These variables are commonly represented by a vector $\mathbf{x} = (x_1, x_2, ..., x_n)$ and some examples are the cross-sectional area and thickness of the structure, the material properties, densities, among others. Within this definition, we can group such variables into two groups: continuous and discrete. Continuous design variables acquire any value within a certain range where intermediate values are considered. Discrete design variables are characterized by their specific values, i.e., integer values. Binary variables are an example of this class as only

values 0 or 1 are considered in the optimization.

- Objective function: The objective functions are employed in order to determine the performance of the structure. Stresses, stiffness, design cost and weight are parameters commonly used as objective functions. Optimization problems are defined in uni-objective – when only a determined function $f(\mathbf{x})$ is considered – or in multi-objective – when more than one function $f(\mathbf{x}) = [f_1(\mathbf{x}), f_2(\mathbf{x}), f_3(\mathbf{x}), ..., f_n(\mathbf{x})]$ is used.

- Constraints: The design needs are bounded by the constraint functions. In this way, the constraints correspond to an imposed parameter which must be satisfied by the problem. Constraints can be classified into two types: inequality constraints $g(\mathbf{x})$, which specifies upper and lower values for design variables and equality constraints $h(\mathbf{x})$ set when a specific value must be reached.

1.3.1 Problem formulation

The general design optimization problem is formulated as

$$
\begin{aligned}
\underset{\mathbf{x}}{\text{Minimize}} \quad & f(\mathbf{x}) \\
\text{Subject to} \quad & g_i(\mathbf{x}) \leq 0 \quad \forall \, i \in [1, \, N_g] \\
& h_b(\mathbf{x}) = 0, \quad \forall \, b \in [1, N_e] \\
& \mathbf{x}_j \in \{0, \, 1\} \quad \forall \, j \in [1, \, N_d].
\end{aligned}
\tag{1}
$$

where $\mathbf{x}$ corresponds to the design variables vector of size N_d, $f(\mathbf{x})$ is the objective function, $g_i(\mathbf{x})$ represents the inequality constraints and $h_b(\mathbf{x})$ the equality constraints. N_g and N_e are the number of inequality and equality constraints in the problem, respectively. In this work, the design variables $\mathbf{x}_j$ are restricted to 1 and 0 since a binary method is adopted. The TOBS method is employed to solve the optimization problem and will be described in the next chapters for each case studied.

1.4 List of publications

Two publications were generated from this research which are listed below.

- P1 – K. E. S. Silva, R. Sivapuram, S. Ranjbarzadeh, R. S. Gioria, E. C. N. Silva and R. Picelli. Topology optimization of stationary fluid–structure interaction problems including large displacements via the TOBS-GT method. Structural and Multidisciplinary Optimization, 65:337, 2022, DOI: `https://doi.org/10.1007/s00158-022-03442-3` – article replicated with the permission of the journal.

- P2 – K. E. S. Silva, R. Sivapuram, K. Ku, J. Labaki, G. H. Yoon and R. Picelli. Structural foundation design via topology optimization and soil-structure interaction – To be submitted to International Journal for Numerical and Analytical Methods in Geomechanics.

1.5   Structure of the thesis

This thesis is structured in four chapters that address the main contributions of this research and is divided as follows. In the introductory chapter, the motivation and objectives of this work are presented. An overview of structural optimization along with the list of publications arising from this research are also presented in this chapter. In chapters 2 and 3 the aforementioned publications are reproduced. In both chapters, the introduction of the problem, the formulation and their respective numerical application with the discussions and conclusions are exposed for each case. Thus, chapters 2 and 3 can be read independently. Lastly, chapter 4 addresses the final conclusions of the work and suggestions for futures works.

2 TOPOLOGY OPTIMIZATION OF STATIONARY FLUID-STRUCTURE INTERACTION PROBLEMS INCLUDING LARGE DISPLACEMENTS

2.1 Context

The optimization of fluid-structure interaction problems including large displacements is solved considering a steady-state analysis of flexible structures in contact with a fluid flow governed by the incompressible Navier-Stokes equations. The optimization framework employed in this work, named TOBS (Topology Optimization of Binary Structures) with geometry trimming (TOBS-GT), consists of an extension of the standard TOBS method [18] which considers the physical analysis and optimization module in a decoupled form. The decoupled analysis allows the finite element problem to be meshed and solved accordingly to the physics requirements. Optimized geometry is constructed by reading and trimming out from an optimization grid described by a set of binary $\{0, 1\}$ design variables. Displacements are resolved using an elastic formulation with geometrical non-linearities to allow for large deformations. The FSI system is solved by using finite elements and the Arbitrary Lagrangian-Eulerian (ALE) method. The sensitivities are calculated using semi-automatic differentiation and interpolated to optimization grid points. In order to consider large displacements, a mapping between material and spatial coordinates is used to identify and track the deformed configuration of the structure. To the best of author's knowledge, this is the first work to employ binary design variables in FSI problems including large displacements and has been published in *Structural and Multidisciplinary Optimization* [20].

2.2 Introduction

Fluid-structure interaction (FSI) is a very common multiphysics phenomenon in nature, present in different proportions and areas of application [21, 22, 23, 24]. Despite occurring in different degrees and forms, the FSI problem is present in several engineering systems such as engines, acoustics, turbines, pumps and others. In these systems, FSI plays an important role and influences design decisions [13, 25]. However, systems involving FSI problems are known for their high complexity, which makes structural designs challenging and highly non-intuitive. Thus, structural optimization methods emerge as a crucial ally for the development of projects with better performance in terms of stability, stiffness and economic aspects.

Topology optimization methods have become popular in fluid-structure systems being applied to a variety of problems [26, 27, 28]. Compared to parametric and shape optimization, topology optimization allows non-intuitive solutions to be generated from a full domain regardless of the initial configuration and have been adopted in several engineering areas [10, 29]. In general, topology optimization involving multiphysics systems face higher challenges compared to the optimization of a single physics. A fundamental point to consider when optimizing FSI problems is the modeling of interface conditions. FSI problems are characterized by the strong coupling between physics, i.e., the structure and the fluid move together and depend on each other [30, 31, 32]. In some cases, the position of the FSI interface is allowed to change during optimization.

This approach is called "wet" optimization. Such an approach is challenging and leads to design-dependent loads, i.e., fluid loads are intrinsically dependent on the structural boundary and can possibly change as the structural design is updated [14, 33]. Thus, it is necessary to adopt precise techniques capable of tracking coupling conditions during optimization. On the other hand, the so-called "dry" optimization does not allow the removal of interface elements and only the internal geometry of the structure is optimized [34, 35]. This work considers the "dry" and "wet" approach and aims to design structures with higher stiffness (minimum compliance) subject to FSI loads allowing for large displacements.

Different approaches have been used to optimize the structural topology in FSI problems. The first work employed a density-based approach. Yoon [36] proposed a SIMP (Solid Isotropic Material with Penalization) unified model that solved both governing equations in a monolithic approach. Later, Yoon [37] applied the same method to stress-constrained problems. Further discussions and comparisons were provided by Lundgaard et al [33] who revisited the same SIMP-based for FSI problems approach proposed by Yoon [36, 37]. In both works, the "wet" optimization was considered. Density-based methods consider an interpolation in the material constant properties between solid and fluid within each element. However, such methods have an unclear structural boundaries during optimization due to the use of intermediate densities elements, which implies a difficult physical interpretation in addition to possible numerical inaccuracies. Jenkins and Maute [35] employed a method based on the explicit level-set for "dry" optimization of FSI problems. A generalized formulation of the extended finite element method (XFEM) was used to track the changes in the structural boundary during the optimization. The same approach was applied for "wet" optimization later on [14]. Picelli et al [38] considered the level-set based approach for fluid pressure loading problems. Fluid flooding technique was adopted to track changes in the FSI interface during optimization. A different technique for tracking the interface based on the level-set framework was proposed by Feppon et al [39] in the topology optimization of thermal fluid-structure problems. Feppon et al [39] proposed a remeshing method based on the evolution of the level-set function to capture the FSI interface. A new framework which employs reaction–diffusion equations (RDE) to update the level-set function was proposed by Li et al [40]. In such approach, a body-fitted adaptive mesh scheme is employed as a remeshing technique. Level-set methods employ level-set functions that explicitly describe the structural boundaries via iso-contours. The interface FSI is clear and well defined. However, the level-set framework is usually complex and requires minuscious care in the level-set update to guarantee boundary smoothness, adding challenges to the already complex FSI problems.

The clear and explicit distinction between physical boundaries is also provided by binary methods (also called discrete) [41]. Alternatively, binary methods are generally easier to implement compared to level-set methods. Picelli et al [42] addressed the optimization of FSI problems using binary design variables via the BESO (Bi-directional Evolutionary Structural Optimization) method [43]. The fluid and solid domains as well as the governing equations were modeled separately. The BESO method, however, is built upon a heuristic-design update scheme, presenting difficulties when applied to a general optimization problem. Still in the binary class of methods, Picelli et al [15] applied the TOBS (Topology Optimization of Binary Structures)

method in the "wet" optimization case of structures under fluid flow loads. The author developed a new methodology to integrate different optimization and finite element packages. The idea consists in decoupling the binary optimization grid (from TOBS) and the finite element analysis (FEA) mesh. A CAD (Computer-aided Design) model is created by reading the $\{0, 1\}$ variables and trimming the void regions (variables 0) out from the original design domain. This leads to the TOBS with geometry trimming (TOBS-GT) method. Picelli et al [44] showed that the TOBS-GT method can be used to optimize turbulent fluid flow properties. In this work, the idea is extended to show possible benefits in multiphysics optimization as it allows the modeling of separate domains in addition to the possibility of employing conveniently coarse meshes, decreasing the computational costs involved in the FSI simulation. The standard TOBS solver is based on formal mathematical programming which allows the efficient implementation of multiple constraints in the problem [45].

In such context, this work proposes the extension of the methodology based on the TOBS-GT method [15] for optimizing FSI problems including large structural displacements. The TOBS is a gradient-based method and employs sequential linear approximation of objective and constraint functions to generate subproblems associated with integer linear programming (ILP). Despite the effectiveness of the studies and different approaches mentioned above, the consideration of more realistic problems including large structural deformations is still a challenging topic when dealing with FSI problems. Up to date, the design of structures under viscous fluid loads considering large displacements was effectively employed only by Jenkins and Maute [35, 14]. When optimizing FSI problems with large structural deformations, the fluid-structure interfaces must be properly tracked and explicitly defined for sensitivities to be calculated correctly. The binary $\{0, 1\}$ design variables provide clear structures which facilitate the imposition of coupling conditions and the numerical analysis of separate fluid and structural domains. Although FSI problems are commonly transient, herein we carry out the optimization considering a steady-state regime as a design approach, since the computational costs of transient analyzes are still a challenge for topology optimization. In this study, we develop a framework that extends the the TOBS-GT method to efficiently deal with fluid structure design problems considering non-linear structural responses. Compliance minimization is solved subject to a volume fraction constraint. COMSOL Multiphysics is used as FEA package to solve FSI equations and provide semi-automatic symbolic differentiated sensitivities. An optimization grid defined by a set of binary design variables $\{0, 1\}$ is created in the TOBS module. Then, the optimization grid is passed to the FEA module and a geometry file is generated. The geometry is produced by reading the set of discrete variables, where $\{1\}$ represents the solid domain and $\{0\}$ is the void or fluid regions. The trimmed geometry is freely meshed with the FEA package. The problem is solved in the spatial (Eulerian) and material (Langragian) frame, thus allowing the map between the optimization point coordinates and the calculation of the sensitivity field in the deformed position. Fluid loads are linearly interpolated via the stress-equilibrium coupling condition. The TOBS-GT method is applied to design of 2D and 3D structures under viscous fluid flow loads. To the best author's knowledge, this is the first work to employ binary topology optimization to design FSI systems including large displacements. The remainder of the paper is as follows. Section 2.3 describes the FSI model used in this work: the Navier Stokes equations (Section

2.3.1), the structural mechanics (Section 2.3.2) and the coupling conditions at the interface (Section 2.3.3). The optimization problem is described in Section 3.4 including details from the TOBS and TOBS-GT methods and the computational procedure. 2D and 3D numerical examples are presented and discussed in Section 2.6. The paper is concluded in Section 2.7.

2.3 Fluid-structure interaction

We consider a steady-state analysis of elastic structures in contact with viscous incompressible fluid. In this work, the fluid flow is modeled in a Eulerian (spatial) frame while the solid structure is modeled in a Lagrangian (material) frame. The fluid flow is considered to be laminar and is governed by the incompressible Navier Stokes and continuity equations. Moving mesh is considered and structural non-linear responses are evaluated.

2.3.1 Navier-Stokes equations

An incompressible viscous fluid flow in constant motion (as illustrated in Fig. 4) is governed by the Navier Stokes and continuity equations [46]. Considering a steady-state incompressible homogeneous Newtonian fluid, the equations are given by

$$\rho_f \left(\mathbf{v} \cdot \nabla \right) \mathbf{v} = \nabla \cdot \left[-P\mathbf{I} + \mu_f \left(\nabla \mathbf{v} + (\nabla \mathbf{v})^{\mathrm{T}} \right) \right] \qquad \text{on } \Omega_f, \tag{2}$$

$$\rho_f \nabla \cdot (\mathbf{v}) = 0 \qquad \text{on } \Omega_f, \tag{3}$$

where ρ_f is the fluid density, $\mathbf{v}$ is the fluid velocity, P is the fluid pressure, $\mathbf{I}$ is the unit diagonal matrix and μ_f is the fluid dynamic viscosity. Equation 2 corresponds to the momentum equation
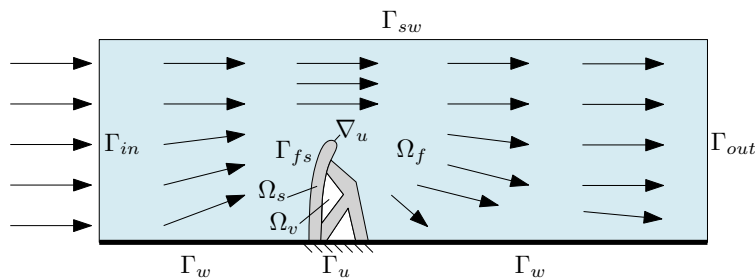
Figure 4: A schematic illustration of the FSI problem.

in an Eulerian formulation of reference, i.e., spatial frame. The terms on the left side of the equation are due to convective acceleration and the right side represents the internal forces in the fluid (inertial forces and viscous forces). The fluid inertial and viscosity forces are related by the Reynols number Re, where $\text{Re} = \text{F}_{inertial}/\text{F}_{viscous}$. Equation 3 expresses the incompressibility of the fluid. In order to solve the governing fluid equations, the following boundary conditions are imposed:

$$\mathbf{v} = \mathbf{v}_0 \qquad \text{on } \Gamma_{in}, \tag{4}$$

$$[-P\mathbf{I} + \mu_f \left(\nabla \mathbf{v} + (\nabla \mathbf{v})^{\mathrm{T}}\right)]\mathbf{n}_f = -\hat{P}_0 \mathbf{n}_f \qquad \text{on } \Gamma_{out}, \tag{5}$$

$$\hat{P}_0 \leq p_{out} \qquad \text{on } \Gamma_{out}. \tag{6}$$

The inlet flow condition (Eq. 4) is prescribed the at the channel boundary Γ_{in}. At the outlet of the fluid channel Γ_{out} a stress free condition is applied (Eq. 5 and 6), where $\mathbf{n}_f$ is the unit normal vector outward to the fluid and p_{out} is the pressure at the outlet of the channel. A slip condition ($\mathbf{v} \neq 0$) is imposed on the flow walls prescribed with Γ_{sw}, on the walls Γ_w and on the interface Γ_{fs} are assumed non-slip conditions ($\mathbf{v} = 0$).

2.3.2 Structural mechanics

The solid domain Ω_s (see Fig. 4) is computed in a Lagrangian frame [47, 48]. All the discrete equations are derived with respect to the original configuration of the structure (undeformed position). This formulation is commonly called Total Lagrangian formulation. In this approach, a displacement vector $\mathbf{u}$ is used to account for the displacements from each material point $\mathbf{X}$ to a spatial point $\mathbf{x}$. Thus

$$\mathbf{x} = \mathbf{X} + \mathbf{u}, \tag{7}$$

where $\mathbf{x}$ is the spatial coordinate, $\mathbf{X}$ is the material coordinate and $\mathbf{u}$ is the displacement vector. The deformation gradient tensor $\mathbf{F}$ can be introduced to report the deformation of an infinitesimal line element $\mathrm{d}\mathbf{X}$ in the material domain to a deformed line element $\mathrm{d}\mathbf{x}$ in the spatial domain as

$$\mathrm{d}\mathbf{x} = \frac{\partial \mathbf{x}}{\partial \mathbf{X}} \mathrm{d}\mathbf{X} = \mathbf{F}\mathrm{d}\mathbf{X}, \tag{8}$$

Therefore, $\mathbf{F}$ can be written as

$$\mathbf{F} = \frac{\partial \mathbf{x}}{\partial \mathbf{X}} = \nabla_{\mathbf{u}} + \mathbf{I}, \tag{9}$$

where $\nabla_{\mathbf{u}}$ is the displacement gradient given by the derivatives of the deformed coordinates with respect to the initial coordinates. The strain state is evaluated in the material configuration by the Green-Lagrange strain tensor given by

$$\mathbf{E} = \frac{1}{2}(\mathbf{C} - \mathbf{I}), \tag{10}$$

where $\mathbf{C} = \mathbf{F}^{\mathrm{T}}\mathbf{F}$ is the right Cauchy-Green deformation tensor. The tensors $\mathbf{E}$ and $\mathbf{C}$ do not contain rigid body strains. The strain tensor $\mathbf{E}$ can be rewrite using the displacement gradient $\nabla_{\mathbf{u}}$ as

$$\mathbf{E} = \frac{1}{2}[(\nabla_{\mathbf{u}})^{\mathrm{T}} + \nabla_{\mathbf{u}} + (\nabla_{\mathbf{u}})^{\mathrm{T}}\nabla_{\mathbf{u}}], \tag{11}$$

where the higher order term $(\nabla_{\mathbf{u}})^{\mathrm{T}}\nabla_{\mathbf{u}}$ corresponds to the non-linear character. The equilibrium state is described in terms of the 2nd Piola-Kirchhoff stress tensor $\mathbf{S}$ defined as

$$\nabla \cdot (\mathbf{FS}) + \mathbf{f}^{fsi} = 0, \tag{12}$$

where $\mathbf{f}^{fsi}$ is the vector of fluid loads applied on the structure, i.e., at the interface Γ_{fs}. The stress tensor $\mathbf{S}$ can be related with the Cauchy stress tensor $\boldsymbol{\sigma}_s$ via

$$\boldsymbol{\sigma}_s = \mathbf{JFSF}^{\mathrm{T}}, \tag{13}$$

where $\mathbf{J}$ is the Jacobian matrix. Once the material is considered to be isotropic and linearly elastic, the linear constitutive relation between the stress tensor $\mathbf{S}$ and the strain tensor $\mathbf{E}$ can be expressed by the Saint-Venant Kirchhoff elastic constitutive equation which is stated by

$$\mathbf{S} = \lambda_s(\mathrm{tr}\mathbf{E})\mathbf{I} + 2\mu_s\mathbf{E}. \tag{14}$$

where λ_s and μ_s are Lamé constants. This constants can be described in terms of the Young's modulus E and Poisson's ratio ν as

$$E = \frac{\mu_s(3\lambda_s + 2\mu_s)}{\lambda_s + \mu_s}, \tag{15}$$

$$\nu = \frac{\lambda_s}{2(\lambda_s + \mu_s)}. \tag{16}$$

In order to solve Eq. 12, Dirichlet boundary conditions are applied at Γ_u as

$$\mathbf{u} = 0 \qquad \text{on } \Gamma_u. \tag{17}$$

2.3.3 Coupling interface

The coupling between solid domain and fluid domain at the FSI interface is defined by the kinematic and stress equilibrium conditions. The kinematic condition concerns the continuity in velocity and the stress equilibrium condition defines the continuity of the interface with respect to the normal vectors of both domains [49]. The stress coupling condition for steady-state is expressed as

$$\boldsymbol{\sigma}_s\mathbf{n}_s = -\boldsymbol{\sigma}_f\mathbf{n}_f \qquad \text{on } \Gamma_{fs}. \tag{18}$$

where $\boldsymbol{\sigma}_s$ is the solid stress tensor, $\boldsymbol{\sigma}_f$ is the fluid stress tensor, $\mathbf{n}_s$ is normal unit vector outward to the solid and $\mathbf{n}_f$ is normal unit vector outward to the fluid, both in the deformed configuration. A moving mesh is considered in order to evaluate the movement of the fluid-structure interface, i.e., how the structure deforms due to fluid flow loads and how the fluid domain changes due to the movement of the structural boundary. The moving mesh interface in COMSOL Multiphysics employs the Arbitrary Lagrangian-Eulerian (ALE) method which separates the spatial frame (fluid domain) from the material frame (solid domain), enabling the easy identification of changes in physical boundaries. In this way, the solid structure follows the mesh displacement.

2.4 Topology optimization problem

2.4.1 Problem formulation

This study concerns the structural mean compliance minimization subject to a volume fraction constraint. The mathematical formulation of the problem considering binary variables $\{0, 1\}$ can be stated as

$$
\begin{aligned}
& \underset{\boldsymbol{\rho}}{\text{Minimize}} \; C(\boldsymbol{\rho}) = \frac{1}{2} \mathbf{f}^{\mathrm{T}} \mathbf{u} \\
& \text{Subject to } V(\boldsymbol{\rho}) \leq \overline{V}, \\
& \qquad \rho_j \in \{0, 1\}, \; j \in [1, N_d],
\end{aligned}
\tag{19}
$$

where $\boldsymbol{\rho}$ represents the vector of design variable ρ_j, $C(\boldsymbol{\rho})$ is the structural mean compliance or total deformation energy, $\mathbf{f}$ and $\mathbf{u}$ corresponds to the loads vectors and the global structural displacement respectively, V is the total material volume of the structure, $\overline{V}$ is the prescribed structural volume fraction and N_d is the number of elements in the design variable vector.

2.4.2 Material models

In order to evaluate the derivatives of the structural mean compliance, the physical model should be interpolated with the design variables. We adopted the SIMP material model which is expressed as

$$
E(\rho_j) = \rho_j^p E_0 \qquad \text{on } \Omega_s,
\tag{20}
$$

where $E(\rho_j)$ is the interpolated material property with respect to the design variable ρ_j, E_0 is the Young's modulus of the solid element and p is the penalty exponent factor. We also adopted a linear material interpolation in order to couple the sensitivities with the fluid loads that change during optimization with the material removal from the fluid-structure interface. Thus, the Eq. 18 referring to the stress equilibrium condition is rewritten as

$$
\boldsymbol{\sigma}_s \mathbf{n}_s = -\rho_j \boldsymbol{\sigma}_f \mathbf{n}_f \qquad \text{on } \Gamma_{fs}.
\tag{21}
$$

More information and discussions about the effects of this material model are given in the numerical results (Sec. 2.6).

2.4.3 TOBS method

The standard TOBS method generates optimization subproblems via sequential linear approximation. Since binary design variables $\{0, 1\}$ – 0 for void and 1 for solid material – are employed, the TOBS framework solves the linear optimization subproblems using integer linear programming (ILP). Therefore, in order for the design variables to remain integer and binary during optimization and the ILP problem to be satisfied, changes in the design variables are constrained by means of a bounded constraint described by

$$
\begin{cases}
0 \leq \Delta \rho_j^k \leq 1 & \text{if } \rho_j^k = 0, \\
-1 \leq \Delta \rho_j^k \leq 0 & \text{if } \rho_j^k = 1,
\end{cases}
\tag{22}
$$

where $(\cdot)^k$ indicates the value of quantity $(\cdot)$ at iteration k and $\Delta\boldsymbol{\rho}^k$ is the vector of changes in the design variables. To keep the binary nature of problem the changes in the design variables are restricted. Therefore, for a solid element ($\rho_j = 1$) the possible changes are $\{0\}$ or $\{-1\}$ which remains solid or becomes void, respectively. For void elements the same definition is valid, where $\{0\}$ is prescribed to remain void element or $\{1\}$ to become a solid element. The optimization subproblems are generated applying Taylor's series approximation and truncating at the linear terms. The objective and constraint functions can be rewritten as

$$C(\boldsymbol{\rho}) \approx C(\boldsymbol{\rho}^k) + \frac{\partial C(\boldsymbol{\rho}^k)}{\partial \boldsymbol{\rho}} \cdot \Delta\boldsymbol{\rho}^k + O(\left|\left|\Delta\boldsymbol{\rho}^k\right|\right|_2^2),$$
$$V(\boldsymbol{\rho}) \approx V(\boldsymbol{\rho}^k) + \frac{\partial V(\boldsymbol{\rho}^k)}{\partial \boldsymbol{\rho}} \cdot \Delta\boldsymbol{\rho}^k,$$
(23)

where $O(\left|\left|\Delta\boldsymbol{\rho}^k\right|\right|_2^2)$ represents the truncation error. There is no error associated with the volume function because its variation is linear. In Eq. 23 the higher order terms for the mean compliance function are neglected since the ILP problems are created using linear approximation. This implies that, for the approximation to be valid, the truncation error needs to be small enough. For this, an extra constraint is added to constrain the number of changes to the design variables in each iteration. This constraint can be expressed as

$$\left|\left|\Delta\boldsymbol{\rho}^k\right|\right|_1 \leq \beta N_d.$$
(24)

In the context of topology optimization, the β parameter guarantees that only a fraction of the total number of variables evolves from solid $\{1\}$ to empty $\{0\}$ and vice versa in each iteration. Therefore, the adoption of small β values is essential for the truncation error to be small enough.

Thus, the linearized optimization subproblem can be written as

$$\underset{\Delta\boldsymbol{\rho}^k}{\text{Minimize}} \ \frac{\partial C(\boldsymbol{\rho}^k)}{\partial \boldsymbol{\rho}} \cdot \Delta\boldsymbol{\rho}^k,$$
$$\text{Subject to} \ \frac{\partial V(\boldsymbol{\rho}^k)}{\partial \boldsymbol{\rho}} \cdot \Delta\boldsymbol{\rho}^k \leq \overline{V} - V(\boldsymbol{\rho}^k) := \Delta V^k,$$
$$\left|\left|\Delta\boldsymbol{\rho}^k\right|\right|_1 \leq \beta N_d,$$
$$\Delta\rho_j^k \in \{-\rho_j^k, 1 - \rho_j^k\}, \ j \in [1, N_d],$$
(25)

where $\Delta\rho_j^k$ is the update of the kth design variable corresponding to the jth element and ΔV^k is the upper limit of the volume constraint. Solving the ILP problem, the design variables are updated as

$$\boldsymbol{\rho}^{k+1} = \boldsymbol{\rho}^k + \Delta\boldsymbol{\rho}^k.$$
(26)

As mentioned earlier, the linear approximation of functions is only valid for small changes in the objective and constraint functions at each update of the design variables. However, some of the problem's constraints can start in an infeasible space due to the bound $\Delta V_i^k = \overline{V} - V(\boldsymbol{\rho}^k)$ requiring a big step to reach a viable solution. Since the topology change is restricted to each iteration by the β parameter, the upper bounds of the constraints ΔV^k are relaxed to generate

feasible ILP subproblems. The constraint bounds are relaxed using

$$\Delta V^k = \begin{cases} -\epsilon_i V\left(\boldsymbol{\rho}^k\right) & : \overline{V} < (1 - \epsilon_i) V\left(\boldsymbol{\rho}^k\right), \\ \overline{V} - V\left(\boldsymbol{\rho}^k\right) & : \overline{V} \in [(1 - \epsilon_i) V\left(\boldsymbol{\rho}^k\right), (1 + \epsilon_i) V\left(\boldsymbol{\rho}^k\right)], \\ \epsilon_i V\left(\boldsymbol{\rho}^k\right) & : \overline{V} > (1 + \epsilon_i) V\left(\boldsymbol{\rho}^k\right), \end{cases} \tag{27}$$

where ϵ_i is the relaxation parameter corresponding to the volume constraint. Effectively, the parameter ϵ gradually limitates the constraint functions moves towards their upper bounds ensuring that a viable solution exists at each iteration.

The ILP problem (Eq. 25) originated from the sequential linearization of functions is the same as a linear programming (LP) problem, however ILP problems are restricted to integer design variables. Therefore, ILP-based solutions can be slightly below the solutions generated by LP problems. However, the structural design obtained by ILP solutions have a clear and well-defined boundary/interface due to the use of integer variables. A famous technique used to solve ILP problems is the branch-and-bound algorithm. In this technique, the ILP problem is initially solved as an LP problem, i.e., without integer constraints. Then, the obtained solution is used as the initial solution and different LPs are created with additional extra limits on the design variables, which forces the optimizer to generate entire solutions in the branches [50]. In this work, we employ the branch-and-bound algorithm present in the CPLEX package to solve the ILP problem generated at each iteration.

2.4.4   Adjoint sensitivities

The TOBS is a gradient-based optimization method, hence the gradients (sensitivities) of the objective and constraint functions are required to iterate over solutions. The respective sensitivities can be calculated using the adjoint method [51, 10]. The general formulation of the adjoint equation for a Lagrangian functional L can be given by

$$\left(\frac{\partial \mathbf{R}}{\partial \mathbf{u}}\right)^{\mathrm{T}} \boldsymbol{\lambda} = -\left(\frac{\partial \mathbf{f}}{\partial \mathbf{u}}\right)^{\mathrm{T}}, \tag{28}$$

where $\boldsymbol{\lambda}$ corresponds to the vector of adjoint variables, f is the vector of objective function and $\mathbf{R}$ is the residual. Sensitivities can then be calculated by the following expression

$$\left(\frac{\mathrm{d}L}{\mathrm{d}\boldsymbol{\rho}}\right) = \left(\frac{\partial \mathbf{f}}{\partial \boldsymbol{\rho}}\right)^{\mathrm{T}} + \boldsymbol{\lambda}^{\mathrm{T}} \frac{\partial \mathbf{R}}{\partial \boldsymbol{\rho}}. \tag{29}$$

The structural mean compliance sensitivities are then calculated by the generic function (Eq. 47). The structural volume sensitivities with to respect to the design variable ρ_j are expressed as

$$\frac{\partial V}{\partial \rho_j} = V_j. \tag{30}$$

where V_j is the volume fraction referring to the design variable j.

2.5 Computational procedures

The proposed method considers the optimizer and problem physics in a decoupled way, i.e., as independent modules. A geometry trimming procedure and interpolation of sensitivities are used to integrate both modules. The proposed optimization method is based on material distribution and built upon the standard TOBS method [18]. A diagram illustrating the steps of the algorithm is presented in the Fig. 6. The equilibrium equations of the FSI problem are solved via the finite element method using an external FEA package, herein COMSOL Multiphysics. The equations are computed with a segregated numerical solver, i.e., with separate domains and in a iteratively manner. In addition, the required sensitivities for optimization are also provided by the FEA package. Besides the fluid-structure interaction module used for the physical analysis of the problem in COMSOL Multiphysics, we employed the topology optimization module to include the material model into the design domain. Through the "density model" tool present within the topology optimization module we can define the type of interpolation and the penalty factor as well. Also, the "optimization" module is used to access the semi-automatic built-in symbolic differentiation tool. The interpolation of the material and FSI coupling (Eqs. 20 and 21) is determined by editing the properties in the structural mechanics and multiphysics coupling modules. Sensitivity analysis is performed by the adjoint method and obtained via the semi-automatic built-in symbolic differentiation module integrated in the software. The TOBS approach with geometry trimming (GT), so-called TOBS-GT, uses a grid points of interest described by binary variables $\{0, 1\}$ to communicate with the FEA module. Geometry trimming (GT) method is the process of creating a CAD geometry by reading the design variables provided and trimming out the initial CAD model of the design domain. The procedure reads the binary design variables – which prescribes the presence (1) or absence (0) of material – and generates a CAD model which contains all the contour information of the problem. This procedure is illustrated in Fig. 5.
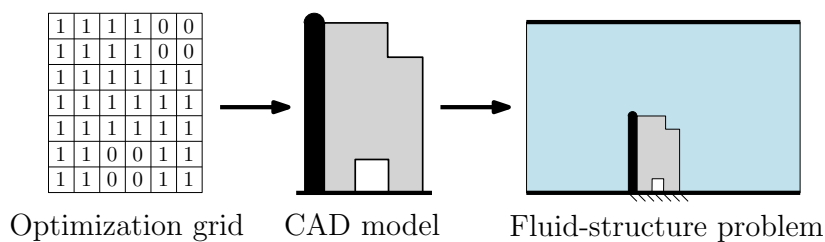
Figure 5: Representation of the geometry trimming (GT) procedure.

A geometry is produced from these contour information (in .dxf, for 2D, or .stl format, for 3D) and transferred to the FEA module via the geometry trimming technique. The optimization grid as well as the .dxf and .stl files are dimensionless. Therefore, a scale factor is applied in order to obtain the actual physical dimension of the problem. The void domains described by variables 0 are trimmed out from the design domain and the CAD file with the respective geometry is updated every iteration. The contour information contains the exact location of the void regions (holes), i.e., whether they are located entirely inside the solid design domain or at the FSI interface. Internal holes are completely trimmed out from the CAD model and holes at the initial FSI interfaces are assigned to be fluid domain. Thus, the FSI interface is directly

tracked and the "fluid flooding" technique as previously used in the literature [52] is not needed. In this work, we do not apply smoothing filters on the FSI interface, so the topologies have a staircase contour. Once the fluid and solid domain is defined, COMSOL Multiphysics are able to identify the boundaries corresponding to FSI interfaces and apply the coupling conditions. The software meshes the geometry freely according to physical requirements. The use of free finite element meshes configured according to physical requirements is advantageous for fluid structure problems, since the mesh quality at the physical boundaries – flow channel walls and FSI interface – are higher, promoting a good approximation of the problem. In this study, this procedure is done using the option `physics controlled` in COMSOL Multiphysics. Triangular and quadrilateral elements are employed. The analyzes are performed assuming plane strain. A quadratic Lagrange approximation is used for the structural analysis and the $P_1 + P_1$ or $P_2 + P_1$ discretization is employed for the fluid flow. FEA is carried out and semi-automatic differentiated sensitivities are computed. The Fluid-Structure Interaction interface in COMSOL Multiphysics employs an arbitrary Lagrangian-Eulerian (ALE) method to account for changes in physical boundaries. The ALE method integrates the fluid flow domain using a spatial frame (Eulerian description) with the solid domain using a material frame (Lagrangian description). The spatial frame is formulated in a system of fixed coordinates in space and the material frame is fixed to the material and moves along with the deformed object. The optimization grid is defined in the material frame and sensitivities are computed in the deformed structural position, as illustrated in Fig. 7. An auxiliary linear analysis is considered in order to avoid convergence problems arising from large local structural displacements due to possible breakage of thin structural members. In summary, the system is analyzed first in the non-linear regime and, if by chance the solver does not converge, we employed a linear analysis in the current iteration in order to re-establish the stability of the structure and move on with the optimization. In this work, linear analysis was activated only in a few iterations, not being necessary in all examples. Furthermore, all problems converged within the non-linear regime.
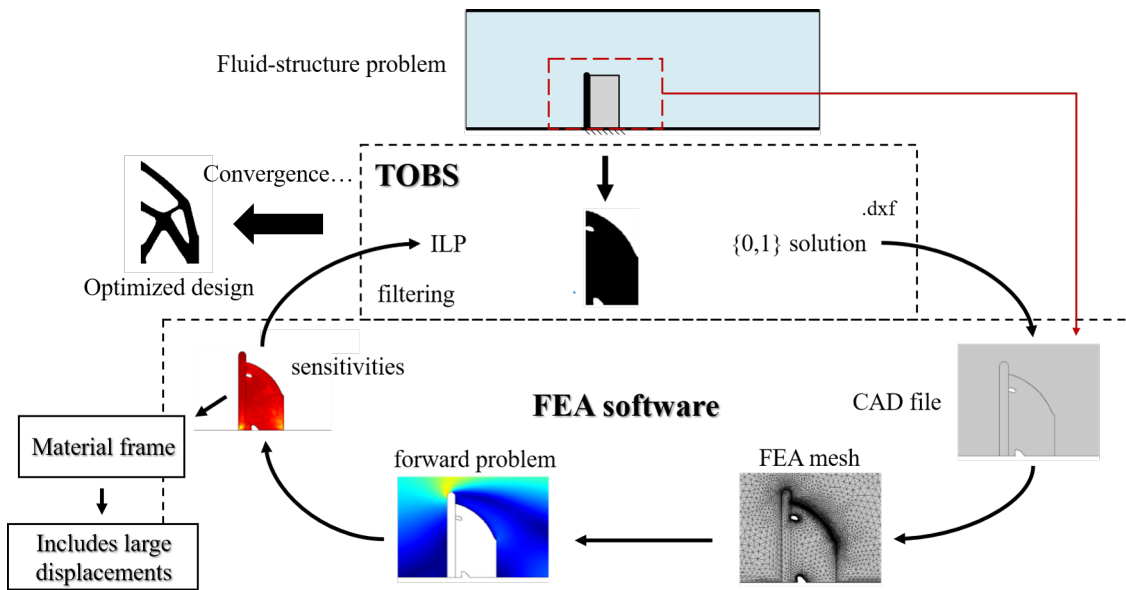
Figure 6: Illustration of the TOBS-GT method for fluid-structure design including large displacements.
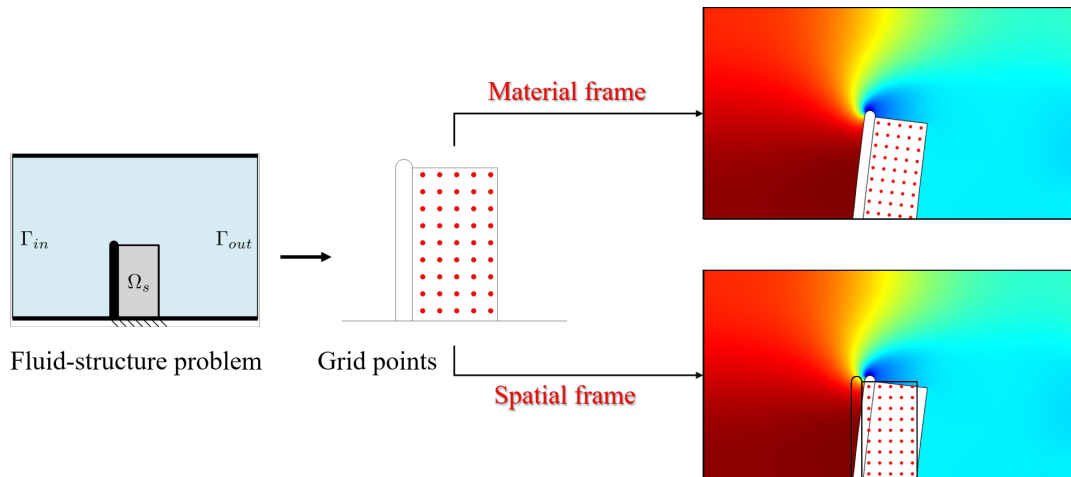
Figure 7: TOBS optimization grid computed in the material frame with mapping to the spatial frame.

The objective function of the structural mean compliance is computed through the expression `solid.Ws_tot` incorporated in COMSOL Multiphysics. The sensitivities of the structural model are integrated in the variable `fsens(dtopo1.theta_c)/dvol`, where `theta_c` is the vector of interpolation variables (Eq. 20 and Eq. 21) and `dvol` is a volume factor variable considered due to the different sizes of the finite elements. The sensitivities computed at each point are extracted through a set of grid points coincident with the optimization grid. In the TOBS module, a spatial filter is applied to the sensitivities to smooth out the problem and avoid numerical problems, such as the checkerboard. With the respective sensitivities the optimizer provides a new set of binary variables $\{0, 1\}$. This process is repeated until convergence. A summary of the main steps for the TOBS-GT approach is presented below:

1. Define the TOBS parameters;

2. Initialize design variables in the TOBS module via the optimization grid $\{0, 1\}$;

3. Generate a CAD geometry in the FEA package by reading the optimization grid variables and trimming out the void regions;

4. Mesh the geometry created by the CAD model;

5. Solve the FSI system governing equations;

6. Compute the semi-automatic differentiated sensitivities in the grid points considering the mapping between the material and spatial frames;

7. Extract the calculated sensitivities and transfer them to the TOBS module;

8. Filter the sensitivity field defined in the grid points;

9. Solve the ILP problem and update the design variables $\{0, 1\}$ in the optimization grid;

10. Evaluate the convergence of the problem. If converged, stop. Otherwise, return to step 3.

2.6   Numerical examples

This section presents the results obtained using the TOBS-GT method. The goal is to minimize the mean compliance of structures under viscous fluid flow loads including large displacements subject to a volume fraction constraint. The first problem is a variation on a well-known example in the literature called "the wall" problem. We solve the problem by optimizing only the internal geometry of the structure, i.e., "dry" optimization. In the second case, the "wet" optimization approach is considered for a second variation of "the wall" example. In order to compare results, in the first two examples the problem is solved considering the small and large displacements. The third problem presents the application of the method in 3D problems. The numerical examples shown in the following sections were computed using the Intel Xeon Silver 4114 - 2x CPU 2.20 GHz - 128GB RAM. In all the examples, the convergence is defined by averaging the changes in the mean compliance function over 6 consecutive iterations for a tolerance of $\tau = 0.001$.

2.6.1   The wall – "Dry" optimization

The first problem consists of a solid wall immersed in a fluid flow rectangular channel, as shown in Fig. 8. In this problem, we analyze the same problem considering small and large displacements for comparison purposes. We seek to optimize the "dry" topology of the wall, i.e., the internal geometry. The properties of the solid material are Young's modulus $E_0 = 400$ kPa and Poisson's ratio $\nu = 0.3$. The fluid density is $\rho_f = 1$ kg/m^3 and dynamic viscosity $\mu_f = 1$ Pa·s. The average inlet velocity is defined by the Reynolds number described by Re $=\rho_f v_{in} D/\mu_f$, where ρ_f is the fluid density, v_{in} is the mean inlet velocity, D is channel height and μ_s is the fluid dynamic viscosity. Herein, we assume Re $= 1$. The flexible solid wall is immersed in a rectangular channel of 6×2 m and it is subject to viscous fluid flow loads. This example is similar to the proposed by Jenkins and Maute [35]. The fluid flow is prescribed with a parabolic velocity profile at the channel inlet described by $\mathbf{v} = v_{in}6(H - y)y/H^2$ where H is the height of the fluid channel and y is the coordinate in the y direction at each point of the inlet. In the outflow a stress free condition is enforced (with $p_{out} = 0$). A non-slip condition is imposed on all walls of the fluid channel. The bottom edge of the structure is fixed; the displacements are $\mathbf{u} = \mathbf{0}$ on this edge. A layer of passive elements (non-design domain) with a thickness of 0.01 m is assumed between the interface and the design domain (see Fig. 8).
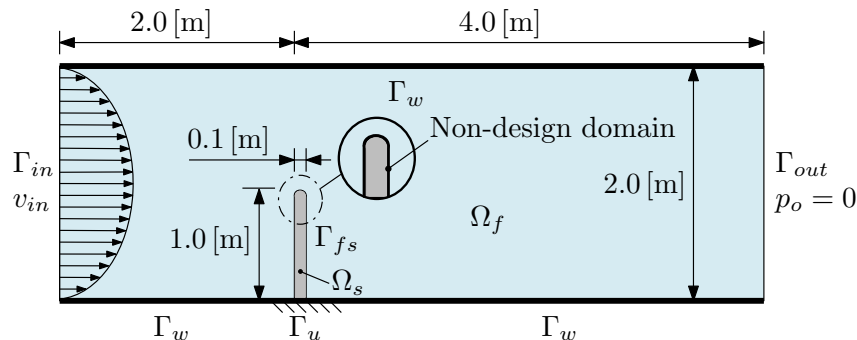
Figure 8: The wall problem: "Dry" optimization.

The internal wall topology is optimized using the TOBS-GT method. The goal of the problem

is to minimize the mean compliance of the structure subject to a volume fraction constraint of $\bar{V} = 60\%$. A 50×500 optimization grid is employed for optimization. A filter radius of 10 grid sizes is adopted. Material model is interpolated considering $p = 3$. The constraint relaxation parameter ϵ is set as 0.01, i.e., the volume function changes 1% at each iteration until it approaches the prescribed volume fraction constraint $\bar{V}$. The truncation parameter – that restricts the percentage of change in design variables at each iteration – is set as $\beta = 0.02$. Figure 9 presents the snapshots of the iterations along the optimization loop for the two cases, the black region represents the solid (1) and the white region corresponds to void (0).

It.: 0   It.: 10   It.: 20   It.: 30   It.: 40   It.: 50   It.: 57
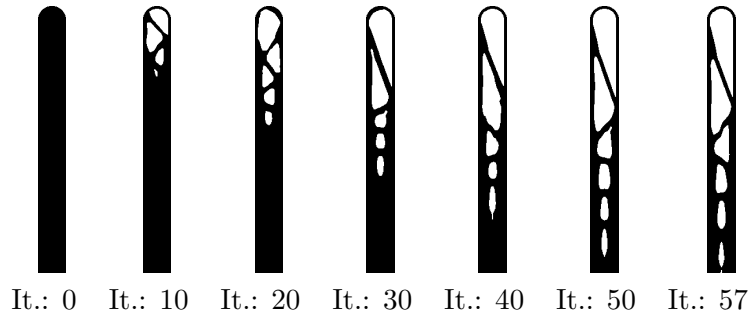
(a) Solution for small displacements

It.: 0   It.: 10   It.: 20   It.: 30   It.: 40   It.: 50   It.: 60
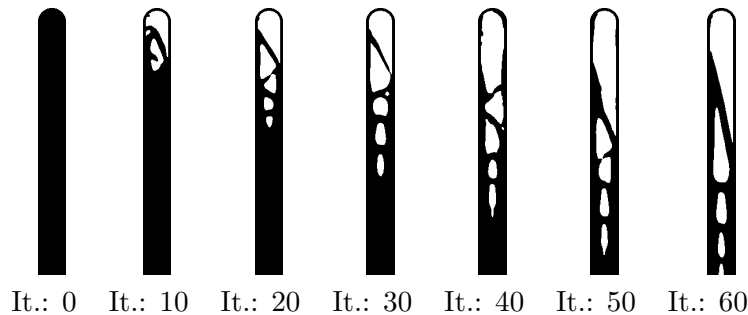
(b) Solution for large displacements

Figure 9: Topology snapshots along the optimization process for the different cases: (a) considering small structural displacements and (b) considering large structural displacements. The black region represents solid (1) and the white region corresponds to void (0).

The inclusion of the structural non-linear response leads to obtaining a different optimized design compared to the linear problem. Figure 9 shows the material distribution within the design domain during the optimization process. Thin bars (similar to a truss) form along the iterations. As expected, the internal arrangement of the bars in the optimized design of each case differs. In the first case – Fig. 9(a) – the optimized design has a larger amount of bars being these of smaller thickness and in the second case – Fig. 9(b) – there are fewer bars with greater thickness. A larger portion of the material is distributed close to the clamped boundary in both cases in order to reduce the overall deformation of the structure. The optimized design obtained for large displacements — Fig. 9(b) – is similar to the topology obtained by Jenkins and Maute [35].

The fluid velocity and pressure fields of the optimized design are plotted in Fig. 10 for the two cases. Velocity profiles and pressure fields are similar in the small and large displacement cases. In general, a greater magnitude in the velocity profile it is just above the structure (see
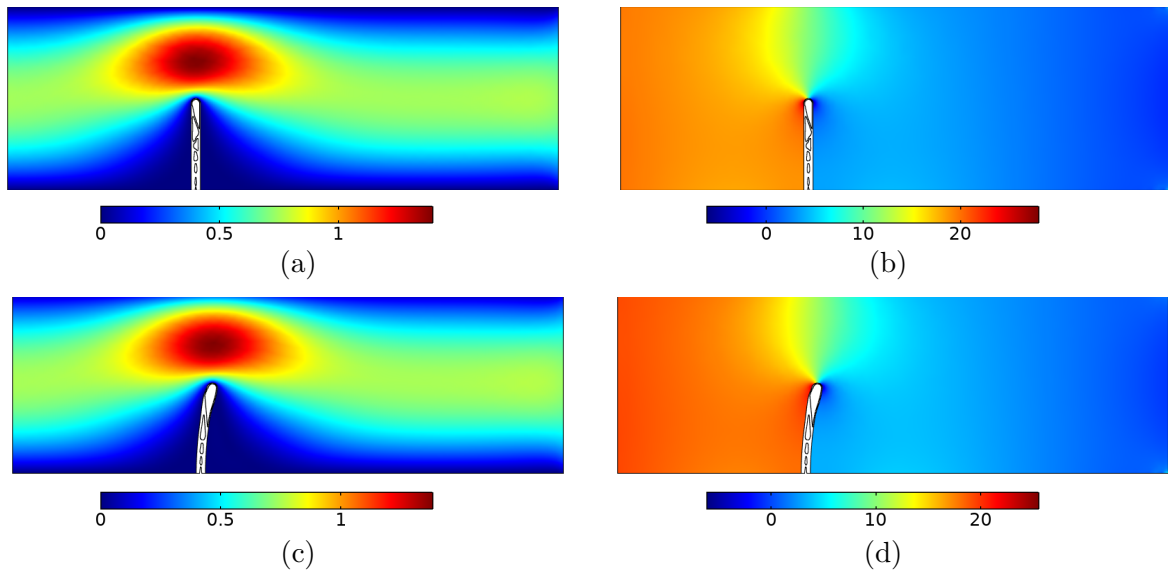
Figure 10: Velocity magnitude (in m/s) and pressure field (in Pa) for the optimized designs: (a-b) considering linear regime and (c-d) considering nonlinear regime.

Figs. 10a and 10c). In the pressure fields – Figs. 10(b) and 10(d) –, it is possible to notice a high positive pressure on the left side of the structure and a significantly lower pressure on the right side, in addition to the existence of a small region of negative pressure coupled in the back of the structure. However, despite the similarity, the case considering small displacements reaches higher pressure values, as shown in Fig. 10(b). In addition, because the FSI interface remains the same along the optimization process, the design obtained for this case would be similar to a case considering a static distributed load – similarly as used in buildings design –, since the fluid loads act as a distributed load over the entire interface of the structure. In the large displacements case, a larger deformation is observed at the top of the structure since the greatest amount of material is distributed at the bottom of the domain. The mapping and distinction between the material and spatial frames in the fluid-structure model allows the TOBS-GT optimization grid to be computed following the deformation of the structure. Structural displacements are computed by the FEA package and the displacement vector is added to the coordinates of the solid material. The optimization grid points are fixed to this frame of reference and the sensitivities are computed accordingly. In this example, the linear interpolation loads does not influence the obtained solutions since only the "dry" topology is optimized, i.e., the solid elements at the interface – in contact with the fluid flow loads – remain in the same position throughout optimization.

The evolution of the objective (mean compliance) and constraint (volume) functions are presented in Fig. 11. As seen in the history of the structural volume fraction, the removal of elements is done gradual as established by the parameter ϵ. It is possible to notice some jumps in the evolution of the objective function in both cases. These punctual increases in the objective function are due to the breakage of the thin bars along the iterations, which causes large local structural deformation, generating a significant increase in compliance, as illustrated in the colorized snapshots with the velocity field presents in Figs. 11a and 11b. However, this behavior does not occur in all cases. The occasional increase in the evolution of the mean
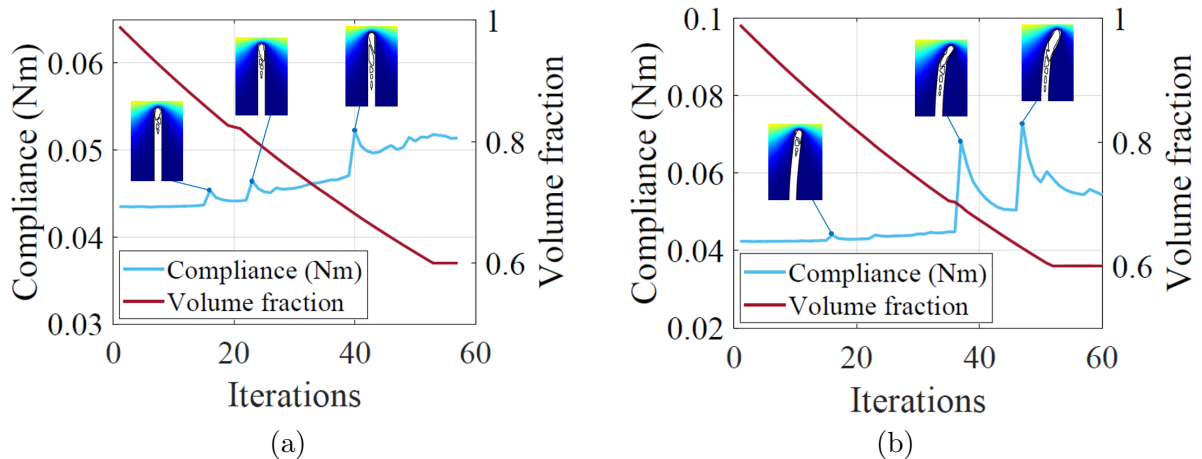
Figure 11: Evolution history of objective function and constraint function for the case considering (a) small displacement and (b) large displacements.

compliance is also observed by Jenkins and Maute [35]. Furthermore, it is interesting to note that with the breakage of the thin bars and consequently the increase in local deformation, the optimizer seeks to add material in order to reduce large deformations and, consequently, minimize compliance. The problem considering small displacements (linear regime) converges to a structural mean compliance value of 0.0514 Nm in 57 iterations. While the final design optimized considering large displacements (non-linear regime) is achieved in 60 iterations with a structural compliance value of 0.0543 Nm.

2.6.2 The wall – "Wet" optimization

In this example, a flexible solid wall is immersed in a fluid flow channel, as shown in Fig. 12. We apply the TOBS-GT method for the optimization of the "wet" topology. This is a classic example of the literature, first proposed by Yoon [36], explored later by other authors [40, 42]. A variation of the problem with a larger design domain was proposed by Lundgaard et al [33]. Herein, we revisit this problem including larger displacements. The objective is to solve the minimization of the structural mean compliance subject to a volume fraction constraint. In comparison to Lundgaard et al [33], we slightly increased the height of the non-design domain bar to obtain larger deformation. The physical properties adopted for the solid domain are Young's modulus $E_0 = 1$ Pa and Poisson's ratio $\nu = 0.3$. The fluid is water, i.e., with density $\rho_f = 1000$ kg/m^3 and dynamic viscosity $\mu_f = 0.001$ Pa·s. The average inlet velocity is defined by the Reynolds number, which is Re = 80.

The fluid flow enters the left edge of the channel with a normal parabolic velocity profile. At the exit of the channel the pressure condition $p_{out} = 0$ is imposed. On the walls of the fluid flow channel a non-slip condition is prescribed. The structure is fixed on bottom boundary, i.e., the displacements are $\mathbf{u} = \mathbf{0}$. The objective of this example is to design an aerodynamic support within a 140×80 mm domain, where a passive region (non-design domain) corresponding to a mid solid barrier is assumed. Structural mean compliance is minimized via the TOBS-GT method subject to final volume fraction of 10%. A 280×160 optimization grid size is used for the design domain. In regard to optimization coefficients, the constraint relaxation parameter
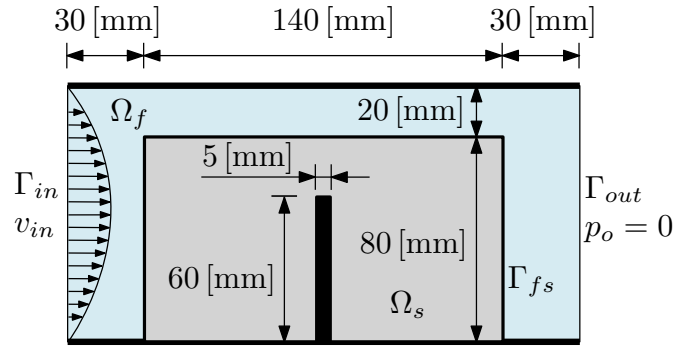
Figure 12: The wall problem: "Wet" optimization.

is set to $\epsilon = 0.02$, the truncation error constraint parameter to $\beta = 0.05$, and a filter radius of 12 grid sizes. The problem is analyzed for small and large structural displacements. Figure 13 presents the topology design, velocity and pressure fields of both cases for the optimized problem using $p = 5$.
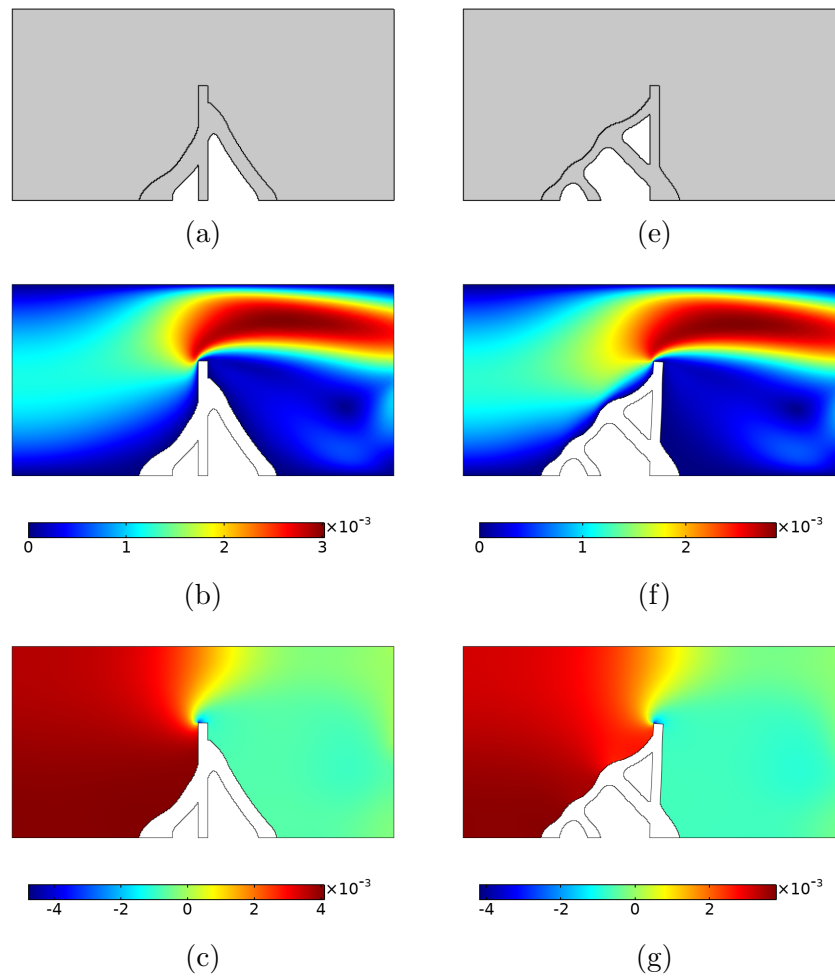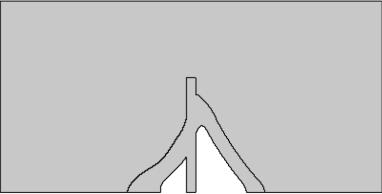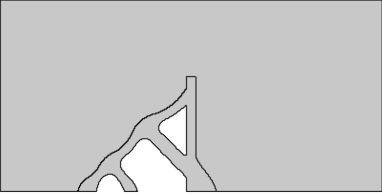
Figure 13: Comparison between the optimized design obtained considering (a-d) small and (e-h) large displacements: (a) and (e) topology design, (b) and (f) velocity magnitude (in m/s), (c) and (g) pressure field (in Pa) using $p = 5$.

It can be noticed that for the large displacement case most of the material is deposited on

the left side of the structure (see Fig. 13e) while in small displacement problem the distribution of solid material within design domain is done in a more balanced way, as seen in Fig. 13a. The velocity and pressure fields differ in the two cases, with higher values observed for the small displacements study. The optimized topology in the small displacement solution is obtained in 122 iterations with the global structural mean compliance value of $1.534 \cdot 10^{-8}$ Nm. A cross-comparison between both designs obtained is presented in the Table 1. Curiously, the design obtained from the optimization including the geometric non-linearity presents a higher performance for both cases, i.e., with and without considering the non-linearities. From this, the advantages of modeling large deformation can be evidenced, but further investigations are necessary to explain why the linear design was not able to find a better solution.

Table 1: Cross-comparison between designs obtained considering small and large displacements.

Designed for / simulated for	Small displacements	Large displacements
Small displacements	$C(x) = 1.5337 \cdot 10^{-8}$ Nm	$C(x) = 1.5290 \cdot 10^{-8}$ Nm
Large displacements	$C(x) = 1.0695 \cdot 10^{-8}$ Nm	$C(x) = 1.1177 \cdot 10^{-8}$ Nm

In order to verify the influence of the penalty factor p, the problem is solved for three different penalty factors $p = \{3, 5, 10\}$ considering large displacements. The velocity and pressure fields are plotted in Fig. 14 for the three cases. It is possible to notice that the optimized structural designs are different for the studied penalty factors. In this model, lower penalty factors favor both stiffness and fluid loading interpolation, while larger penalties decrease considerably the calculation of the fluid loading in the sensitivities. This is also discussed in Yoon [36] and Lundgaard et al [33]. As seen in Fig. 14, more material was deposited on the left side of the structure when lower penalty factors ($p = 3$ and 5) were used. This fact is because with the interpolation of fluid loads, the optimizer is able to work on reducing the high pressure and shear loads arising from the direct contact of the fluid flow with the solid structure. In fact, the structure obtained using $p = 3$ presents the lowest mean compliance value between the

(a) $p = 3$, C(x) = $1.0455 \cdot 10^{-8}$ Nm

(b) $p = 5$, C(x) = $1.0695 \cdot 10^{-8}$ Nm

(c) $p = 10$, C(x) = $1.0990 \cdot 10^{-8}$ Nm
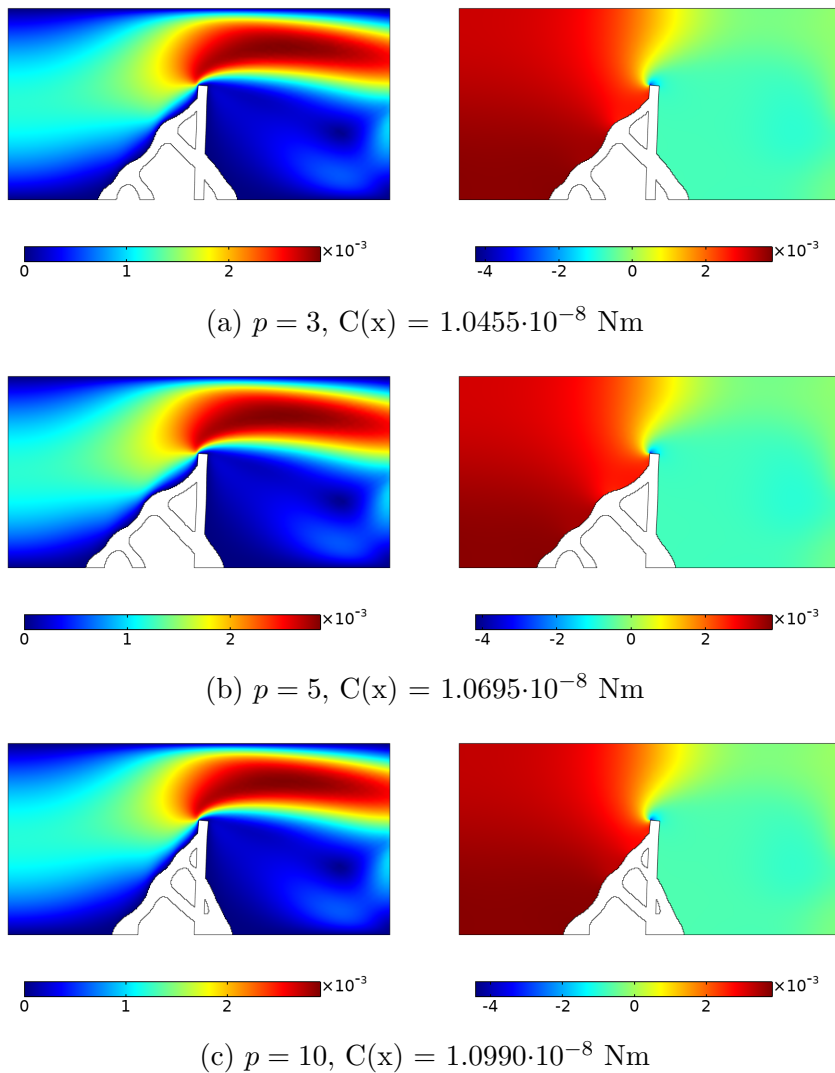
Figure 14: Velocity fields in m/s (left side) and pressure in Pa (right side) of the topology optimized for $p = \{3, 5, 10\}$.

three designs. When solving the problem using $p = 10$, more material was deposited closer to the mid solid wall. Our numerical experience tells that FSI examples with high pressure and shear loads such as this one present convergence difficulties if the fluid loading sensitivities are not used, especially for higher Reynolds number. The structural members in the three designs are arranged to globally reduce the load. The velocity and pressure fields are similar in the three cases. The fluid flow velocity reaches a significant magnitude near the upper region of the intermediate barrier. Besides, the pressure field varies from positive to negative values in after the flow passes the obstacle. Fig. 15 shows the evolution of the topology and velocity profile over the iterations for the case of $p = 5$. As it can be observed during optimization a clear and explicit distinction between physical boundaries – solid and fluid – is obtained along all iterations due to the binary variables.

The evolution history of the mean compliance and volume fraction functions are shown in Fig. 16. The history of the objective function presents some peaks, similarly as in the example of the optimization of the "dry" topology 2.6.1. Sudden increases in compliance were also observed
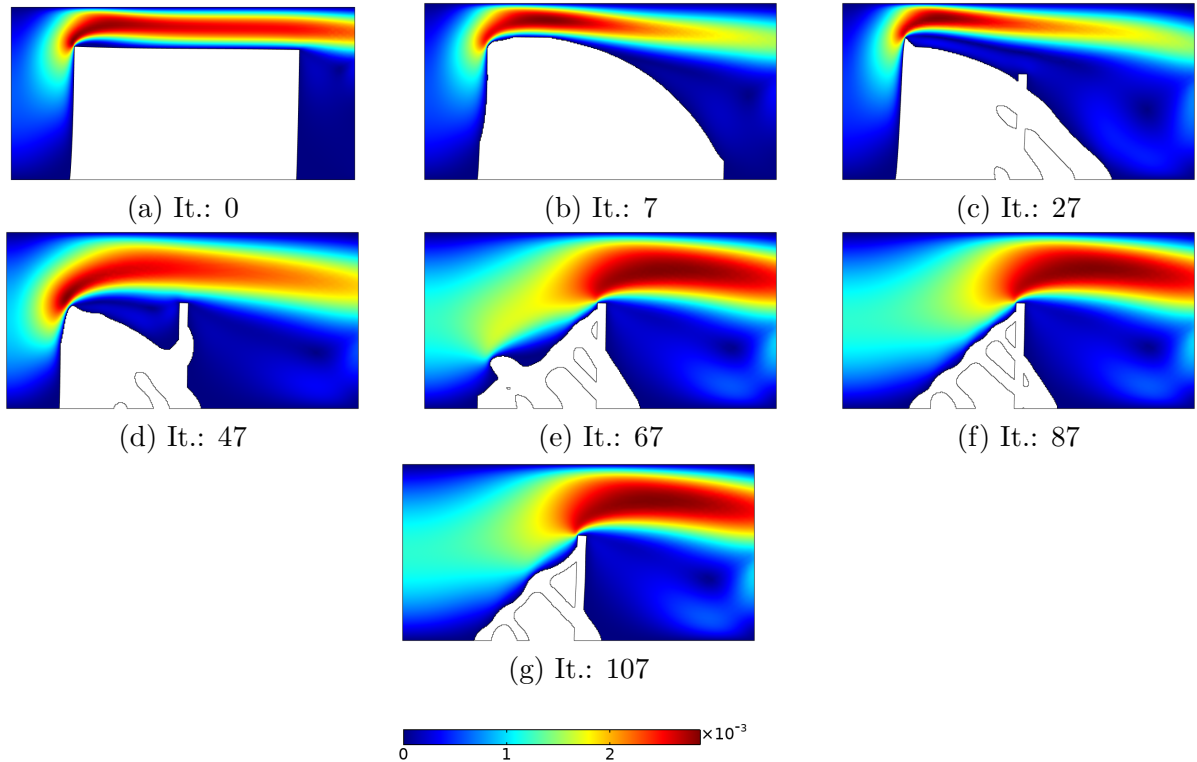
Figure 15: Velocity field (in m/s) of the snapshots during the optimization for $p = 5$.

by Jenkins and Maute [14] in "wet" topology optimization problems. The global measure of structural mean compliance is minimized and the final obtained values are lower than the initial ones. Clear and explicit optimized topologies are obtained. The mesh created by COMSOL Multiphysics for the optimized FSI design using $p = 5$ including the fluid domain is shown in Fig. 17. The area delimited in red represents the initial design domain. The CAD geometry trimming allows the meshes to be freely created, meeting the physical requirements. As it can be noticed, the mesh has a larger discretization in the FSI boundaries and quadrilateral elements are used in the fluid walls. The finite element mesh is composed of 15197 elements – 14637 triangular and 560 quadrilateral elements – while the TOBS-GT optimization grid has 44800 elements ($280{\times}160$ grid points) distributed only in the structural design domain. Mesh refinement is not directly linked to optimization grid size. Therefore, the increase of points in the optimization grid in order to obtain topologies with higher resolution does not lead to a higher computational cost, as the finite element mesh can be kept in a computationally convenient size. The possibility of using coarse meshes in contrast to the higher grid resolution is one of the possible advantages of the TOBS-GT approach. On the other hand, the consideration of a dense FE mesh and a coarse optimization grid should tend to produce smoother fields and, therefore, similar results but with a higher computational cost. The use of coarser meshes reduces the overall time and challenges of the FSI computation, since the bottleneck of the optimization is the finite element analysis. While the FEA solver can take between 20 and 70 seconds each iteration, the ILP problem takes less than 1 second to be computed (see Fig. 18). In addition, the geometry trimming procedure takes on average less than 1 second to be executed as well as the generation of a new FEA mesh at every iteration. Therefore, both processes are significantly

cheap compared to the FEA forward problem. Thus, the TOBS-GT method promises to be relatively cheap for optimizing problems with a high degree of physical complexity.
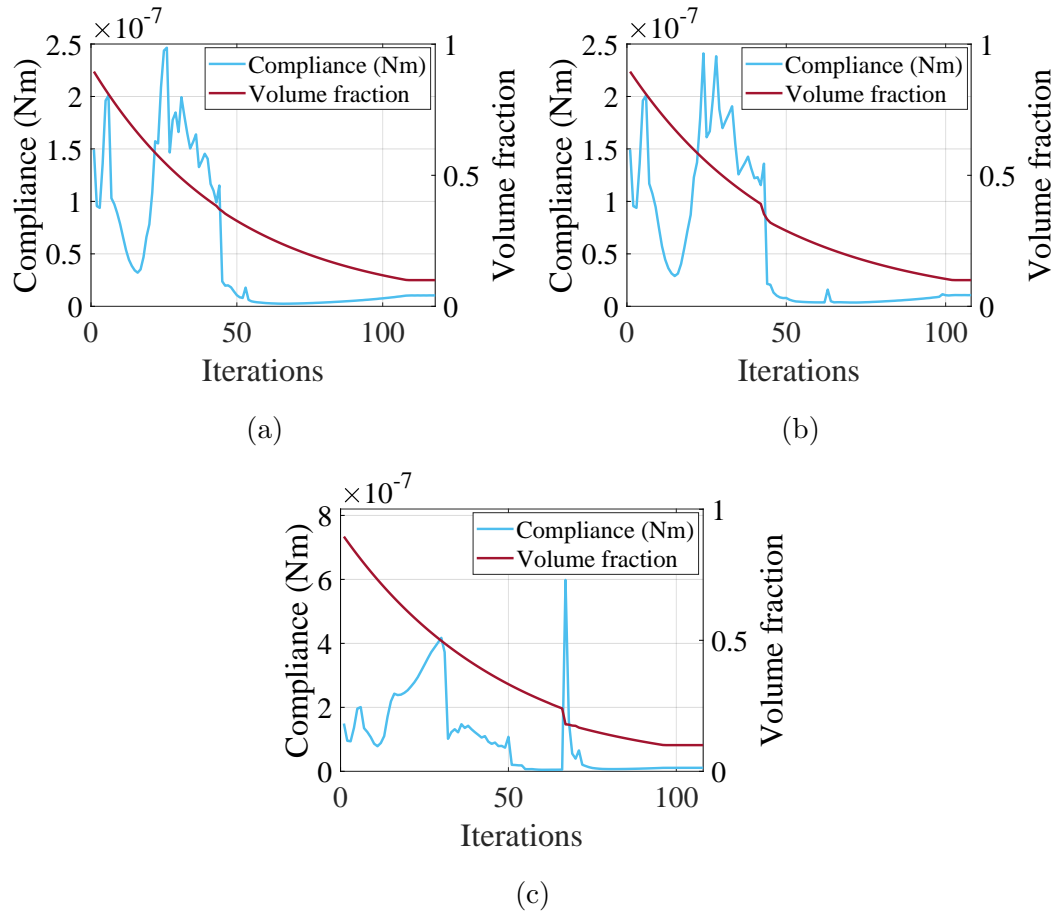
Figure 16: Evolution history of the objective function (mean compliance) and constraint function (volume) for the cases: (a) $p = 3$, (b) $p = 5$ and (c) $p = 10$.
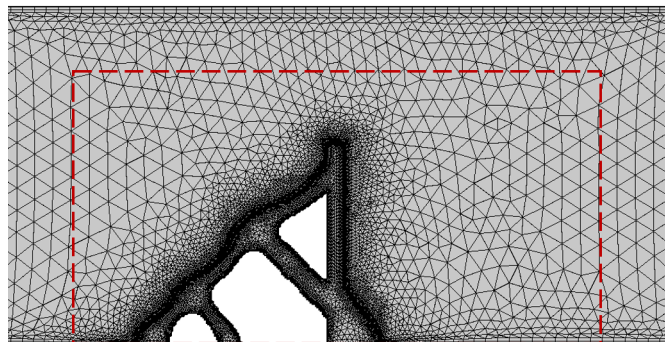
Figure 17: Finite element mesh – 14637 triangular and 560 quadrilateral elements – for the final optimized design ($p = 5$). The red dashed line represents the initial design domain.

2.6.3 The billboard – 3D "wet" optimization

This example solves the "wet" optimization case of a flexible three-dimensional billboard-like structure immersed in a fluid flow channel of dimension $10{\times}6{\times}6$ mm. The problem illustration is shown in Fig. 19. A 0.1 mm thick plate is suspended by a circular main column with a
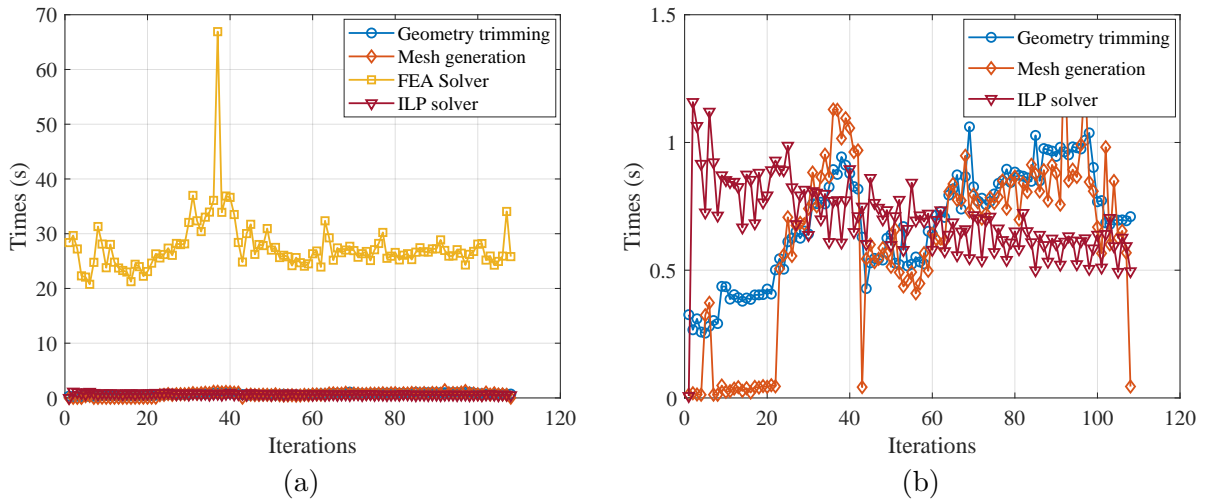
Figure 18: Breakdown computation times of each iteration for the case with $p = 5$ using the TOBS-GT method: (a) for the main optimization steps (b) omitting the FEA solver times.

diameter of 0.33 mm, located on the bottom boundary of the fluid channel and centered on the z–direction , with a distance of 3.0 mm from the inlet Γ_{in}. The objective of this example is to design a support structure behind the suspended plate. The design domain Ω_s is located behind the structure and is connected to the main column at a height of 2.0 mm, and has a dimension of $3\times2\times0.5$ mm. The solid material properties for this example is chosen to have Young's modulus $E_0 = 4\cdot10^3$ Pa and Poisson's ratio $= 0.3$. Fluid is considered to be air (density $\rho_f = 1.27$ kg/m^3 and dynamic viscosity $\mu_f = 1.72\cdot10^{-5}$ Pa·s). Maximum inlet velocity v_{in} is defined to 0.01 m/s.
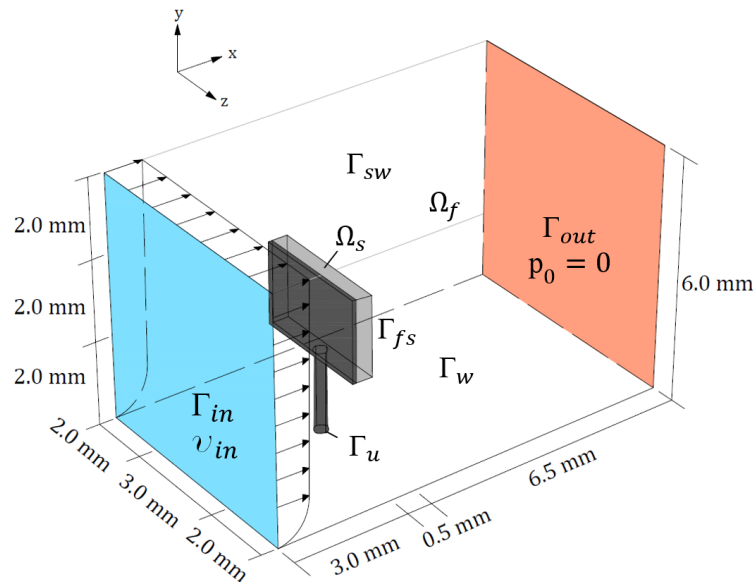
Figure 19: The 3D billboard problem.

A parabolic fluid flow enters the channel Γ_{in} with velocity $\mathbf{v} = v_{in}(y/H)^{\frac{1}{7}}$, where H corresponds to the height of the three-dimensional flow channel – in this case 6.0 mm – and y is the vertical coordinate for each input point. A pressure condition $p_{out} = 0$ is established at the outflow Γ_{out}. The following conditions are imposed on the walls of the fluid channel:

lateral and upper boundaries Γ_{sw} are set to slip condition, lower boundary Γ_w and the fluid-structure interface Γ_{fs} are set to non-slip condition. The displacements in the bottom structural boundary of the main column Γ_u are fixed, i.e, $\mathbf{u} = 0$. The TOBS-GT method is considered to minimize the mean compliance of structural support subject to a volume fraction constraint of $\bar{V} = 30\%$. An optimization grid of size $16{\times}80{\times}120$ is applied and it is located on the back of the board corresponding to the gray region (see Fig. 19). The penalty factor adopted for the material model is $p = 5$. A filter radius of 2 grid sizes is considered. The optimization parameters used are $\epsilon = 0.02$ and $\beta = 0.05$. Some views of the optimized structural design are shown in Fig. 20. The optimized support is connected to the main column of the structure with a greater amount of solid materials being deposited in this region. However, it is still possible to observe the occurrence of large displacements as shown in Fig. 21. The TOBS-GT optimization grid can be placed anywhere of interest in the structure, as in this example where the grid points are considered to be at a height on the y-axis. In this way, any structural component can be optimized using the TOBS-GT approach, as long as the optimization grid $\{0, 1\}$ is placed accordingly. In addition, when considering large displacements, it is important to identify the frame of reference where the points are evaluated. Figure 21 presents the streamlines of the velocity profile for optimized structural support and the zoomed structure in a multislice velocity field plot.

(a)   (b)   (c)

(d)   (e)   (f)
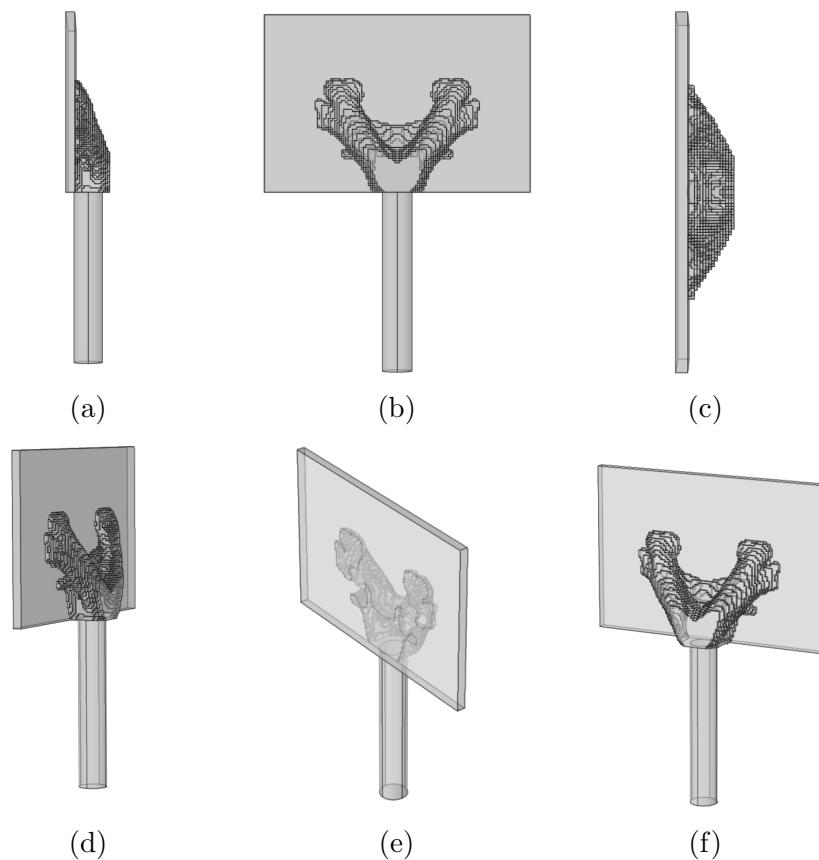
Figure 20: Optimized structural support for 3D FSI problem including large displacements: (a) sideview, (b) back view, (c) top view and (d-f) angled views.
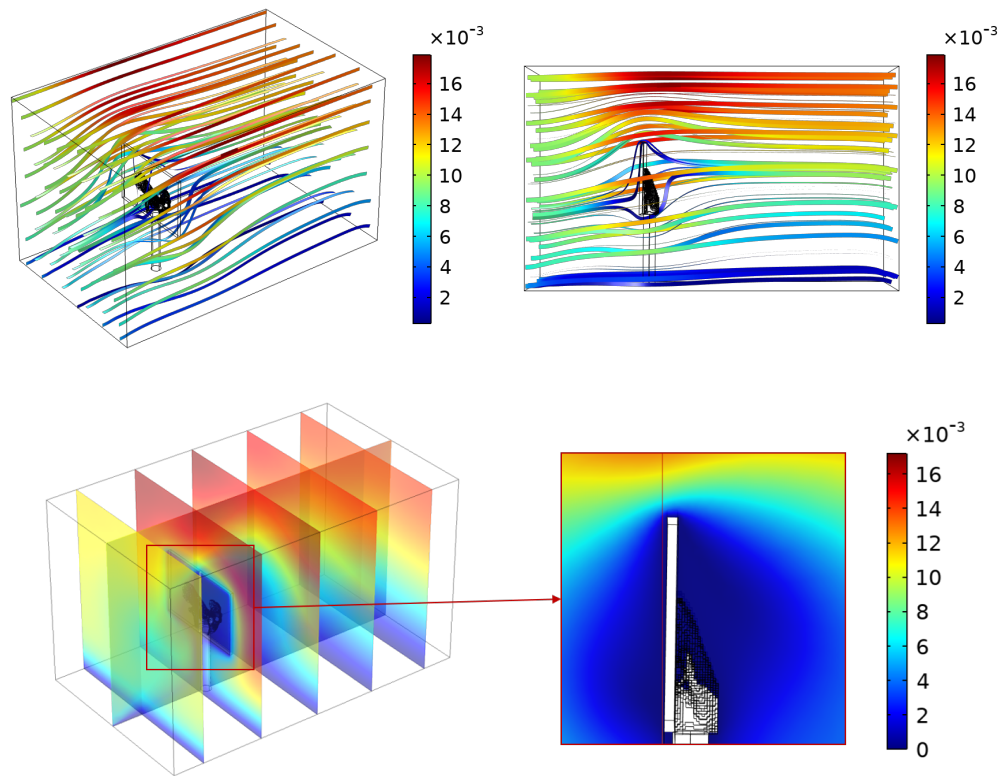
Figure 21: Fluid velocity field (in m/s) around optimized 3D structure via TOBS-GT method.

2.7 Conclusions

A spatial-material framework is employed to extend the TOBS-GT method [15] for optimizing FSI problems including large displacements. The optimized design of structures under viscous fluid loads is achieved through a decoupled analysis, where the optimization grid and the physical analysis are used as independent modules. This approach shows to be convenient when modeling two different physics, such as in the present FSI problem. A decrease in the total number of finite elements used is achieved if compared to the fixed optimization grid size. Thus, the optimization of the FSI topology is performed with a reasonably lower computational cost. The approach, named the TOBS-GT method, integrates the standard TOBS solver Picelli [18] with an external finite element analysis package. For considering large structural displacements, the FSI system is computed in the spatial (Eulerian) and material (Langragian) frame which allows the identification and tracking of the deformed FSI interface. The solid domain is solved using an elastic formulation with geometrical non-linearities. The cases of "dry" and "wet" optimization are solved. Different solutions are obtained when comparing small and large displacements studies. The extension of the proposed methodology to 3D structures is direct. The inclusion of material non-linearity, wall smoothing for high Reynolds numbers and the extension of the present methodology to non-FSI problems – such as single physics problems and multi-material problems – are possible directions for future research.

3 STRUCTURAL FOUNDATION DESIGN VIA TOPOLOGY OPTIMIZATION AND SOIL-STRUCTURE INTERACTION

3.1 Context

To design structural foundations two different materials are considered in the design domain: soil and structural foundation material. Classic topology optimization methods consider only one material within the design domain, generally characterized by solid-void. The inclusion of more than one material, in this case, provides a larger design domain space in addition to optimizing both soil and structural elements since the deformation is transferred through both domains. The soil-structure system is solved by using the Finite Element Method and dynamic loads are considered. A large domain of soil is modeled and PML's (Perfectly Matched Layers) are applied to simulate the unbounded soil for the dynamic case. The sensitivities of the problem are solved via the adjoint method and the materials are interpolated and each one of them is represented by a binary variable. To the best of the author's knowledge, this is the first work to employ binary topology optimization in structural foundations designs considering static and dynamic loads.

3.2 Introduction

Structural solutions with better performance are continuously sought out in the area of structural engineering. The design of complex structures is a challenge and requires adequate tools for its elaboration. Optimization methods have been constantly employed in several engineering areas aiming at the development of ideal designs, taking into account economic aspects and the necessary performance requirements. Despite the large potential, optimization methods are rarely applied in geotechnical field, such as in the design of structural foundations. The application of numerical methods aimed at the optimized models generates more accurate layouts with improved functionality which is advantageous for obtaining innovative structures.

The foundation is an important structural element that aims to support the structural system and properly distribute the loads acting on it to the ground [53, 54]. Structural optimization in foundations design can provide optimized layouts with higher performance to support the loads imposed on the structural system, in addition to lower material usage. Topology optimization (TO) is a powerful numerical method that provides an effective structural layout and can be applied to different types of structures [10, 29, 55]. This optimization approach provides the generation of optimized designs from initial filled domains which allows the entire structural layout to be optimized considering an objective function and prescribed design constraints. However, obtaining optimized layouts in foundation systems is still an underexplored area, especially into TO framework. Most of the studies related to foundation designs are focused on other optimization approaches. Huang and Hinduja [56] employed a nonlinear unconstrained optimization technique to optimize the shape of a machine tool foundation with the objective of reducing the design cost. Still in the shape optimization approach, Sienkiewicz and Wilczyński [57] proposed a sequential programming method to optimize a rectangular machine foundation.

The structure was optimized in order to minimize the weight (mass) of the concrete block subject to a dynamic loads. The lower usage of material in the elaboration of geotechnical designs is a very discussed topic since the cost-benefit is a prerequisite of extreme relevance in the design of these structures [54, 58]. Other approaches were applied to optimize the foundation designs. Juang and Wang [59] employed a genetic algorithm for multi-objective optimization of a robust design of spread footings. The authors minimized the probability of failure of the structure described by the standard deviation of the system response. An approach using a genetic algorithm was also proposed by Hui et al [60]. The optimized design cost of a strip foundation was obtained considering the bending resistance, shearing resistance and detailing requirements ruled by specification as a constraint condition. The genetic algorithms are heuristic approaches based on the biological evolution [61, 62]. Despite the great potential and diverse applicability, genetic algorithms are not based on formal mathematics, which makes them sensitive to initial conditions in addition to the lack of guarantee of obtaining properly optimized solutions. Besides, the high number of objective functions evaluation might make genetic algorithms unpractical when a Finite Element Analysis (FEA) is required.

In the TO field, Grabe and Pucker [63] applied the Solid Isotropic Material with Penalization (SIMP) method to optimize the volume of piled raft foundations. The SIMP is a density-based method that considers intermediate design variables through an interpolation among the constant properties of the material. The SIMP method is quite popular and has been applied to many optimization problems. However, unclear structural boundaries are obtained during the optimization process due to elements with intermediate densities. Later, Seitz and Grabe [64] obtained optimized topologies for some other basic geotechnical problems. The structural topology of a retaining wall, a pile and a strip footing were optimized. Subsequently, the method was extended to applications in 3D problems [65], where the authors proposed the optimization of a 3D shallow foundation in a granular soil. Zied et al [66] employed an optimization approach based on direct limit analysis to optimize shallow and deep foundation designs considering materials governed by Coulomb's failure law. Continuous and discrete designs were obtained. However, in the case of discrete designs, some intermediate densities are still observed due to limitations of the discrete design algorithm used in that work. In addition, the authors considered the use of two materials in the optimization problem: soil and foundation structural material. The inclusion of more than one material in the problem of optimizing geotechnical structures proves to be advantageous and necessary. The classic TO approach considers only one type of material in the optimization process, generally characterized by solid-void. The inclusion of two materials during the optimization process requires the adoption of robust numerical methods, which are capable of capturing the boundaries of each material in a distinct way during the whole process. Binary methods are a good alternative for this type of problem since only binary variables (also called discrete) are considered in the problem. In this way, ill-defined boundaries are avoided during the optimization process.

In this context, this work presents a new methodology to address structural foundations design via a binary approach. We consider the soil-structure interaction into the optimization problem. In this way, two materials with specific properties (soil and structural foundation material) are present in the design domain. For that, the TOBS (Topology Optimization of

Binary Structures) method [18] is adopted. The TOBS is a gradient-based method that employs binary design variables {0,1} and considers sequential integer linear programming to find the optimized structural layout. In addition to avoiding possible numerical inaccuracies, the use of binary design variables provides fully discrete optimized structures due to the clear distinction among the boundaries of the specific materials existent in the design domain, which allows for greater accuracy in the interpretation of the layouts obtained. The TOBS method has already been successfully applied in multimaterial topology optimization problems [67]. Therefore, the method shows great potential to efficiently deal with different materials in the context of soil-structure designs.

Up to date, most of the available studies consider only the action of static loads on the design problem. Recently, Sadeghi et al [68] published a work including dynamic loads in design foundations via TO. The authors applied the Covariance Matrix Adaption Evolution Strategy algorithm (CMA-ES) method coupled with the finite element method in order to minimize the vertical displacement in shallow foundations design for static loads and the vertical velocity considering dynamic loads. The CMA-ES algorithm is based on a normal distribution and employ different parameters to find optimized solutions. Heuristic-based methods generally perform well and are easy to implement. However, they may present certain difficulties in the update scheme since they do not employ gradients or higher derivatives. Within this scope, this work proposes the generation of optimized soil-structure designs subject to static and dynamic loads. For the problem considering static loads, two objective functions are considered. We seek to minimize the mean structural compliance of a tower foundation under a soil domain and also the squared difference of the bottom and top displacements of a tower, respectively. In the dynamic case, the objective is to minimize the squared difference of the displacements between the two points (bottom and top point of the tower) considering an external load for a certain frequency. Both problems are solved subject to a prescribed volume fraction constraint. The PML domain is employed to absorb dynamic waves and simulate the infinite domain. The physical problem is solved by using the Finite Element Method. For this, the commercial software COMSOL Multiphysics is employed as FEA package to solve the soil-structure equations and provide semi-automatic differentiated sensitivities. A fixed mesh is used in the design domain and an optimization grid described by variables {0,1} is created by the TOBS module in order to establish the communication between the FEA package and the optimizer. To the best of the author's knowledge, this is the first work to employ strictly binary topology optimization to design structural foundation systems subject to static and dynamic loads.

The manuscript is organized as follows. Section 3.3 presents the basic formulation based on FEA employed to solve the soil-structure interaction problem. In Section 3.4 and 3.5, the topology optimization framework and the numerical implementation are described, respectively. In Section 3.6, the numerical examples are showed and discussed while in Section 3.7 the paper is concluded.

3.3 Governing equations

This section presents the governing equations for the soil-structure interaction problem. The optimization problems presented are assumed in a two-dimensional structure and are related to

linear structural analysis in the static and dynamic regime. Thus, only small displacements are considered.

3.3.1 Static Analysis
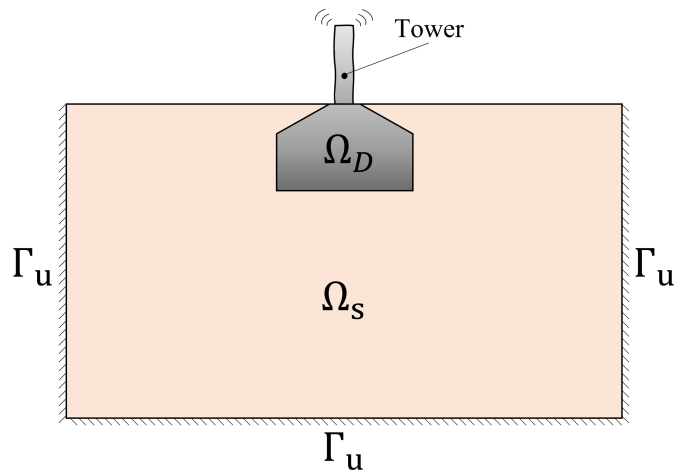
Figure 22: Soil-structure interaction problem – static case.

A linear elastic formulation is assumed in the structural Ω_D and soil domain Ω_s (see Fig. 22). Considering an isotropic domain, disregarding body forces and inertial forces, the linear elastic equation for a continuum medium can be described by

$$\nabla \cdot \boldsymbol{\sigma}_s(\mathbf{u}) = -\mathbf{F} \qquad \text{in } \Omega_D \text{ and } \Omega_s, \tag{31}$$

where $\nabla \cdot \boldsymbol{\sigma}_s$ corresponds to the divergence of the Cauchy stress tensor, $\mathbf{u}$ is the vector of structural displacement and $\mathbf{F}$ is the vector of the external loads acting on the structure.

To solve the Eq. 31, Dirichlet boundary conditions at Γ_u are assumed as

$$\mathbf{u} = 0 \qquad \text{on } \Gamma_u. \tag{32}$$

3.3.2 Dynamic Analysis

Considering the equilibrium of a linear elastic structure in both domains (structural Ω_D and soil Ω_s) – see Fig. 23 – subject to dynamic external loads, the classical momentum equation of the structure system without damping can be stated as

$$\mathbf{M}\ddot{\mathbf{u}}_t + \mathbf{K}\mathbf{u}_t = \mathbf{F}_t, \tag{33}$$

where $\mathbf{M}$ is the structural mass matrix, $\mathbf{K}$ is the stiffness matrix, $\ddot{\mathbf{u}}_t$ and $\mathbf{u}_t$ are the acceleration and displacement vector in the time t, respectively; and $\mathbf{F}_t$ is the external loads acting on the structure related to time t. Given a certain excitation angular frequency ω, the loading $\mathbf{F}_t$ and the displacement $\mathbf{u}_t$ vectors can be expressed as

$$\mathbf{F}_t = \mathbf{F}e^{j\omega t}, \tag{34}$$
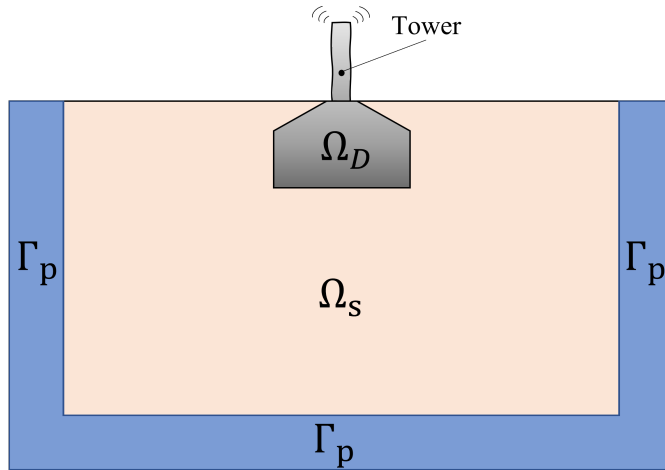
Figure 23: Soil-structure interaction problem – dynamic case.

$$\mathbf{u}_t = \mathbf{u}e^{j\omega t}, \tag{35}$$

where $\mathbf{F}$ and $\mathbf{u}$ are the magnitude of the external excitation load and the displacement, respectively, both vary harmonically and $j = \sqrt{-1}$.

Taking into account only the frequency domain analysis, Eq. (33) can be rewritten in terms of the magnitude of the structural displacement response and the external excitation load as

$$(\mathbf{K} - \omega^2\mathbf{M}) = \mathbf{F} \qquad \text{in } \Omega_D \text{ and } \Omega_s. \tag{36}$$

Eq. (36) expresses the structural equilibrium equation in the frequency domain, which is assumed in the current soil-structure optimization problem. Since the frequency domain analysis addresses the study of the structural response to harmonic steady-state load at a certain frequency ω, all forces and responses consist of complex values. In order to absorb the elastic waves thus avoiding reflections and simulate an infinite domain, PML's are applied to the boundaries Γ_p of the problem.

3.4   Topology optimization problem formulation

3.4.1   Problem Statement

In this work, we address binary $\{0,1\}$ optimization problems subject to a volume constraint. The formulation of the referred problem can be expressed as

$$
\begin{aligned}
\underset{\mathbf{x}}{\text{Minimize}} \quad & f(\mathbf{x}) \\
\text{Subject to} \quad & V_i(\mathbf{x}) \leq \overline{V}_i \quad \forall\, i \in [1,\ N_g] \\
& \mathbf{x}_j \in \{0,\ 1\} \quad \forall\, j \in [1,\ N_d],
\end{aligned} \tag{37}
$$

where $\mathbf{x}$ represents the vector of design variables, $f(\mathbf{x})$ is the objective function, $V(\mathbf{x})$ is the total volume of structural material constrained by a volume fraction prescribed by $\overline{V}$. The number of constraints corresponds to N_g and N_d is the number of design variables present in the problem.

- Objective functions

We seek to optimize the system for two distinct objective functions. First, for the static case, we consider the minimization of the mean structural compliance (also addressed as the mean strain energy of the structure). The mean structural compliance is expressed by

$$C(\mathbf{x}) = \frac{1}{2}\mathbf{F}^{\mathrm{T}}\mathbf{u} = \frac{1}{2}\mathbf{u}^{\mathrm{T}}\mathbf{K}\mathbf{u}, \tag{38}$$

Where $\mathbf{x}$ represents the design variables, $\mathbf{u}$ and $\mathbf{F}$ are the global displacement and load vectors, respectively; and $\mathbf{K}$ is the global stiffness matrix.

In addition, we consider the minimization of the squared difference of the displacements between two points. The points are located at the top and bottom of the structural tower and are indicated by u_1 and u_2. Both displacements are computed vertically in the x-direction and correspond to a scalar value. Thus, the expression can be stated as

$$f(\mathbf{x}) = (u_2 - u_1)^2. \tag{39}$$

where u_1 and u_2 denotes the local displacement in two different points located in the structure. This objective function is used in both static and dynamic cases.

3.4.2 Topology Optimization of Binary Structures (TOBS) method

In order to solve the proposed optimization problem – Eq. (37 –, the TOBS method is employed. The method employs binary {0,1} design variables and resolve the problem via integer sequential linear approximation. Considering the derivatives of the functions (objective and constraint), a sequence of approximate optimization problems (linearized functions) are created and solved using integer linear programming (ILP). The linearization of the objective and constraint functions are generated by the first order Taylor's approximation. Thus, from this, the problem to be solved presented in Eq. (37) is given by

$$
\begin{aligned}
\underset{\Delta \mathbf{x}^k}{\text{Minimize}} \quad & \left.\frac{\partial f}{\partial \mathbf{x}}\right|_{\mathbf{x}^k} \Delta \mathbf{x}^k, \\
\text{Subject to} \quad & \left.\frac{\partial g_i}{\partial \mathbf{x}}\right|_{\mathbf{x}^k} \Delta \mathbf{x}^k \leq \bar{g}_i - g_i(\mathbf{x}^k) := \Delta g_i^k \quad i \in [1, N_g], \\
& \left|\left|\Delta \mathbf{x}^k\right|\right|_1 \leq \beta N_d, \\
& \Delta x_j^k \in \{-x_j^k, 1 - x_j^k\} \quad j \in [1, N_d] \; k \in [1, \; N_m].
\end{aligned}
\tag{40}
$$

where $(\cdot)^k$ indicates the value of quantity $(\cdot)$ at iteration k and $\Delta \mathbf{x}^k$ is the changes in design variables considered for each element j. After each iteration, the design variables are updated as

$$\mathbf{x}^{k+1} = \mathbf{x}^k + \Delta \mathbf{x}^k. \tag{41}$$

To guarantee an ILP problem, bound constraints are imposed on the problem's design variables in order to control changes and ensure that the design variables are always integers

(i.e., 0 or 1) throughout the entire design process. Therefore, the bounded constraints on the design variables are expressed as

$$
\begin{cases}
0 \leq \Delta x_j^k \leq 1 & \text{if } x_j^k = 0, \\
-1 \leq \Delta x_j^k \leq 0 & \text{if } x_j^k = 1,
\end{cases}
\tag{42}
$$

where Δx_j is the changes in design variables considered for each element j. In addition, since a linear approximation is employed, an additional constraint $\left|\left|\Delta \mathbf{x}^k\right|\right|_1 \leq \beta N_d$ is used to avoid large truncation errors and ensure that the linear approximation is valid. In this way, the parameter β is added to the suboptimization problem in order to control the flips in the design variables from 0 to 1 and vice-versa ensuring that the truncation error arising from the Taylor's series approximation remains small.

Since the topology suffers only small changes in each iteration, due to the constraint imposed by the β parameter (Eq. 42), the constraints in the current iteration are subject to a possible infeasibility. Moreover, depending on the initial design domain adopted, it may start in an infeasible space and require a big step to reach a viable solution. To avoid this, the upper bounds of the constraints Δg_i^k are modified so that the optimization subproblem obtain feasible solutions. The constraint bounds are thereby modified by

$$
\Delta g_i^k = \begin{cases}
-\epsilon_i g_i\big(\mathbf{x}^k\big) & : \overline{g}_i < (1 - \epsilon_i) g_i\big(\mathbf{x}^k\big), \\
\overline{g}_i - g_i\big(\mathbf{x}^k\big) & : \overline{g}_i \in [(1 - \epsilon_i) g_i\big(\mathbf{x}\big), (1 + \epsilon_i) g_i\big(\mathbf{x}^k\big)], \\
\epsilon_i g_i\big(\mathbf{x}^k\big) & : \overline{g}_i > (1 + \epsilon_i) g_i\big(\mathbf{x}^k\big),
\end{cases}
\tag{43}
$$

where ϵ_i consists of the relaxation parameter related to the constraint function. In this way, the constraint function is relaxed by moving the upper bounds slowly so that there is always a feasible solution at each iteration.

The integer suboptimization problems – Eq. 40 – arising from sequential linearization of functions (objective and constraint) can be solved using Integer Linear Programming (ILP). The ILP problems use additional constraints in order to keep the design variables always integer, such constraints are what differentiates the problem from a LP problem. Therefore, ILP problems generates suboptimal solutions with respect to the Linear Programming (LP) problems. Thus, since two materials are considered in the optimization problem, the use of integer variables can be beneficial and considerable. The branch-and-bound algorithm present in the CPLEX package – developed by IBM – is employed to solve the ILP problem. In this method, the initial solution is generated from a LP problem (without considering any integer constraints). From this, different LP problems are generated by adding extra constraints to design variables, which forces the optimizer to obtain integer solutions in the branches.

3.4.3 Material interpolation scheme

The optimization problem is modeled assuming more than one material in the design domain. The modified SIMP interpolation is employed in order to carry out the interpolation between the different materials present in the soil-structure problem. Thus, considering two specific materials

(soil and structural material) in the optimization problem, the modified SIMP interpolation is expressed as

$$E(\mathbf{x}_j) = E_{soil} + x_j^p(E_{structure} - E_{soil}), \quad x_j \in [0, 1], \tag{44}$$

$$\rho(\mathbf{x}_j) = \rho_{soil} + x_j(\rho_{structure} - \rho_{soil}), \quad x_j \in [0, 1]. \tag{45}$$

where x_j is the density of the material for the design variable j, $E_{structure}$ and $\rho_{structure}$ are the Young's modulus and density of the foundation material, respectively; and E_{soil} and ρ_{soil} denotes the soil material properties, being the Young's modulus and the density, respectively. The properties are interpolated based on the decision variable x_j which indicates the material property for each finite element in the design domain mesh, being either structural material (variable 1) or soil material (variable 0).

3.4.4 Sensitivity analysis

The TOBS is a gradient-based method, therefore, the derivatives of the objective/constraint functions are necessary to solve the optimization problem (Eq. 40). Such derivatives, also called sensitivities, can be obtained through the adjoint method [10, 51]. The generic formulation of the adjoint equation for a Lagrangian functional L is expressed as

$$\left(\frac{\partial \mathbf{R}}{\partial \mathbf{u}}\right)^{\mathrm{T}} \boldsymbol{\lambda} = -\left(\frac{\partial f}{\partial \mathbf{u}}\right)^{\mathrm{T}}, \tag{46}$$

where $\boldsymbol{\lambda}$ refers to the adjoint variables vector, f is the objective function and $\mathbf{R}$ is the residual. Sensitivities can then be solved by

$$\left(\frac{\mathrm{d}L}{\mathrm{d}\mathbf{x}}\right) = \left(\frac{\partial f}{\partial \mathbf{x}}\right)^{\mathrm{T}} + \boldsymbol{\lambda}^{\mathrm{T}}\frac{\partial \mathbf{R}}{\partial \mathbf{x}}. \tag{47}$$

The sensitivities of the objective functions are obtained by the generic function – Eq. (47). The sensitivities of the constraint function (volume) depends on the structural volume which is defined as

$$V = \sum_{j=1}^{N_d} x_j V_j, \tag{48}$$

where x_j and V_j are the design binary variable and the volume fraction, respectively; both referring to the variable j. Therefore, the structural volume sensitivities related to the design variable x_j are expressed as

$$\frac{\partial V}{x_j} = V_j. \tag{49}$$

3.5 Numerical Implementation

The proposed approach employs the TOBS algorithm presented in `www.github.com/renatopicelli/tobs` and in Picelli et al. [45] coupled with an external FEA package. Unlike the classic TO problems, in this work two different materials are considered in the design domain. The equilibrium equations of both problems (static and dynamic case) as well as the problem's

sensitivities are solved by using the commercial software COMSOL Multiphysics.

3.5.1 Semi-automatic differentiated sensitivities

A stationary study solver built into the sensitivity module in COMSOL Multiphysics is employed to solve the forward problem. Once the software solves the finite element problem, the objective function referring to the displacement difference between two points can be directly written and computed in the software. The objective function of the structural mean compliance is computed via the expression `solid.Ws_tot`, which corresponds to the total elastic strain energy of the structure. Sensitivity analysis is performed by the adjoint method (47) and solved via the semi-automatic built-in symbolic differentiation module integrated in the software. The sensitivities of the problem can be accessed via `fsens(dtopo1.theta_c)/dvol`, where `fsens` corresponds to the software-built expression used to compute the sensitivity (derivative) of the objective function with respect to the specified variable, `theta_c` is the vector of interpolation variables described by x_j – Eq. 44 and 45) – and `dvol` corresponds to a volume factor variable. The computed sensitivities are passed to the optimizer through a set of points coincident with the grid of optimization points. In order to avoid numerical problems and smooth the problem, a spatial filter is applied to the sensitivities field in the TOBS module.

3.5.2 Coupling with external FEA software

The integration between the optimizer and the external FEA package is established through the interpolation of the problem's sensitivities. A grid points of interest described by binary variables $\{0, 1\}$, herein named as optimization grid, is created by the optimizer and then passed to the software. The optimization grid is set in the design domain so that each grid point corresponds to a mesh element. For that, different types of elements are used in the problem. In the design domain, a quadrilateral fixed mesh is employed. The same type of mesh is used in the PML's domain in the dynamic case. The other domains are freely meshed using triangular finite elements. The material distribution is carried on through the interpolation between the materials using interpolation shown in Eq. (44) and (45). The sensitivities required for the optimization problem are solved employing the semi-automatic differentiation module present in the FEA software. The computed sensitivities are provided to the TOBS module and then the ILP problem is solved. From that, a new optimization grid described by a new set of binary variables $\{0, 1\}$ is generated and passed to the FEA package. Figure 24 presents a diagram with the main steps of the algorithm. The new design variables grid is read by the software and the material properties are interpolated based on this new set $\{0, 1\}$, i.e., the decision variables. Each binary variable represents a specific material, being either $\{0\}$ (material 1) or $\{1\}$ (material 2), as illustrated in Fig. 25. Thus, the full domain is filled by material and void domains are not considered. This process is done using the topology optimization module built into COMSOL Multiphysics. The "density model" feature present in this module allows the set of the material interpolation type as well as the penalty factor. Thus, each material is correctly distributed in the design domain considering the design variables provided by the optimizer at each iteration.

Since TOBS is a binary approach, intermediate densities are not considered. Therefore, an explicit and exact definition of the boundary of each material is guaranteed. In the dynamic
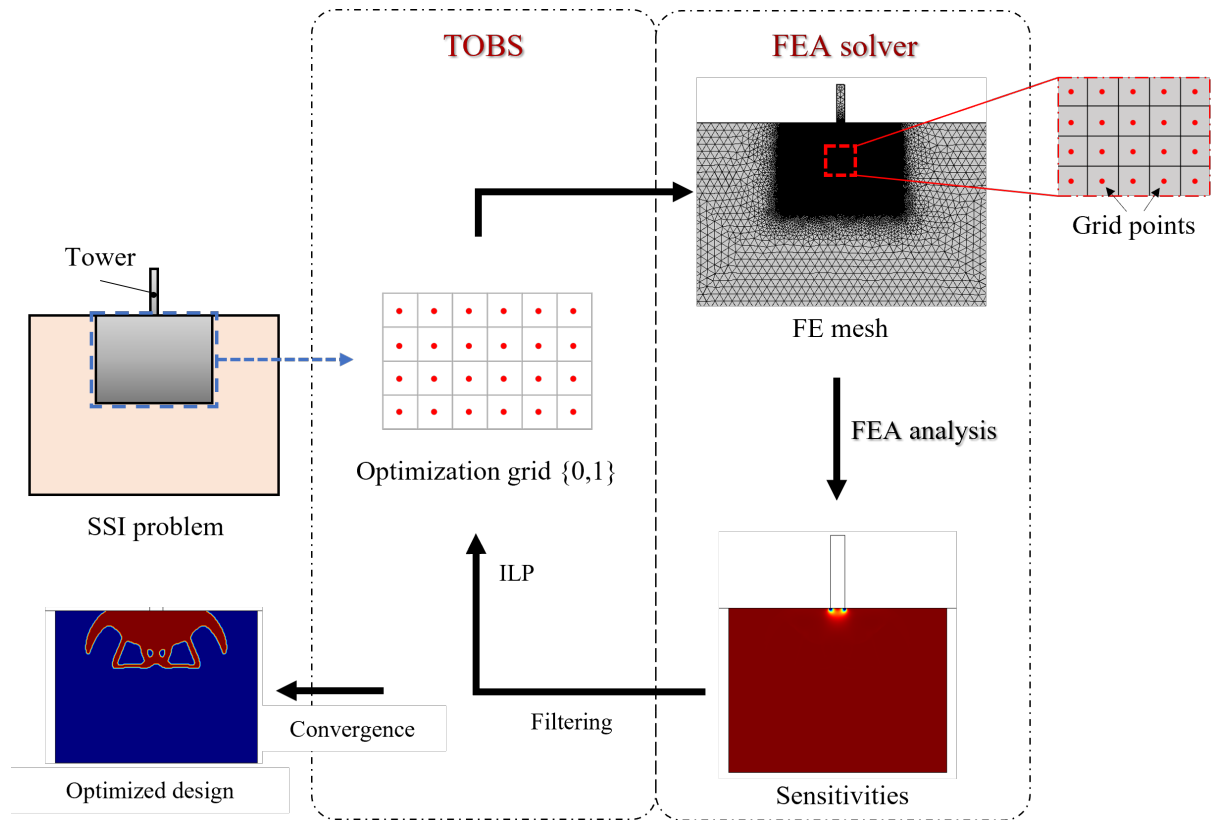
Figure 24: Diagram illustrating the steps of the methodology applied to soil-structure designs.

case, PML's are applied to the domain boundary in order to absorb the elastic waves from harmonic loading. PML's modeling are performed via the artificial domains module integrated to the FEA software. PML settings such as geometry and the coordinate stretching type, the scaling factor and the scaling curvature parameter can be freely edited in the FEA software. In this work, a polynomial geometry is adopted. The scaling factor and the scaling curvature parameter are set to 1 and 3, respectively.

Figure 25: Soil-structure topology based on the TOBS optimization grid.

In summary, the optimization problem solved by coupling between the TOBS method and the external FEA package is performed using the following algorithm:

1. Set the TOBS optimization parameters;

2. Create the optimization grid defined by the design variables {0} or {1};

3. Mesh the design domain with a FE mesh matching the optimization grid;

4. Solve the SSI governing equations;

5. Compute the semi-automatic differentiated sensitivities of the problem in all the TOBS grid points;

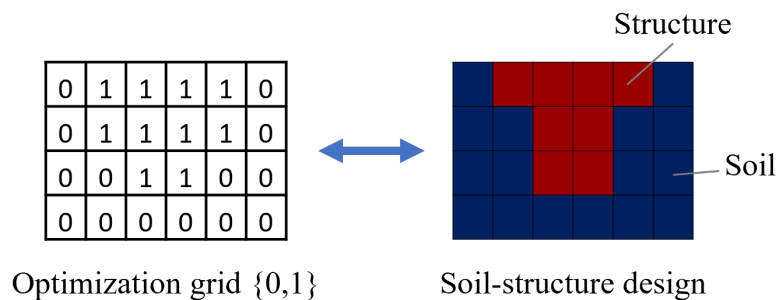6. Compute the objective function;

7. Provide the computed sensitivities to TOBS module and apply spatial filtering;

8. Solve the optimization problem – Eq. 40 – and update the grid optimization described by the design binary variables $\{0, 1\}$;

9. Evaluate the convergence of the problem (objective function and constraints). If the problem converged, stop. Else, return to the step 3.

3.6 Numerical examples

This section presents the numerical results and discussions on the application of the TOBS method in the structural foundations design. First, the problem is solved by considering static loads. In the first example, we seek to minimize the structural mean compliance of the foundation structure, i.e., the maximization of the structural stiffness. Then, all other examples aims the minimization of the squared difference of displacements between the top and bottom points of the above-ground superstructure. First, considering a static loading and, then, a dynamic loading. The second example shows the optimization results for the static loading case. In the first two examples, for the sake of comparison, different initial design domains are explored. In the third example, the tower is subject to a load for a certain frequency. All examples employ a 240×180 optimization grid inside the design domain for the optimization and are subject to a volume fraction constraint. The Poisson's ratio is the same in all the cases and for both materials, $\nu = 0.3$.

3.6.1 Static case

The problem consists of an elastic tower Ω_t of 0.4×5.0 m above a soil domain of dimension 45×25 m. The problem illustration is shown in Fig. 26. Herein, we model a large soil domain in order to simulate an infinite soil medium. The physical property assumed for the tower and foundation domain is Young's modulus $E_f = 3{\cdot}10^9$ Pa and $E_s = 21.5{\cdot}10^6$ Pa for the soil domain. The TOBS method is employed to find the optimized solution of a structural foundation for the tower and is designed within a design domain of dimension 12.0× 9.0 m. We optimize the problem considering a static loading for two cases: minimum structural compliance and minimum squared difference of the displacements between two points. The points are indicated by u_1 and u_2 (see Fig. 26). Both objective functions are subject to a volume fraction constraint of $\bar{V} = 15\%$. A horizontal point load $F = 1000$ N is applied to the center top of the tower. The displacements at the boundary of the soil material Γ_u are fixed, i.e., $\mathbf{u} = \mathbf{0}$.

The TOBS optimization parameter ϵ is set as 0.02, i.e., the volume constraint function changes 2% each iteration until it reaches the prescribed fraction of volume $\bar{V}$. The truncation
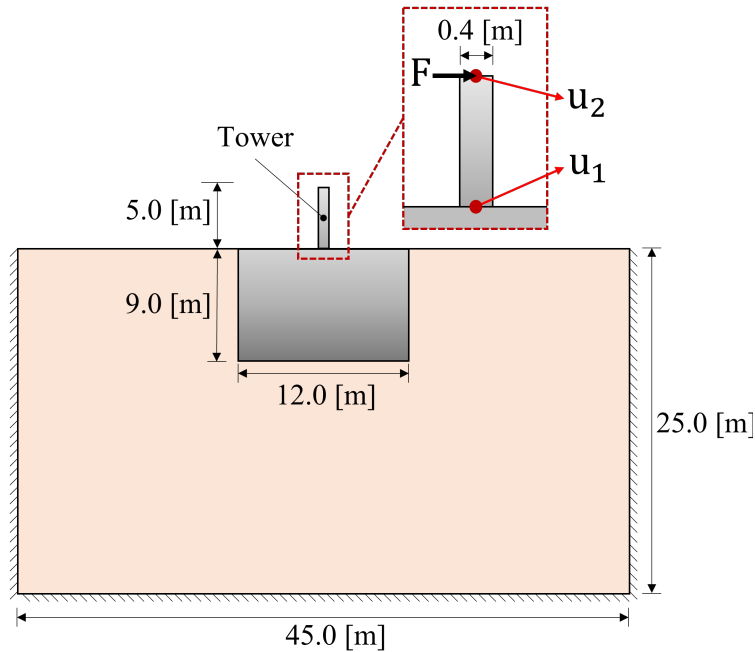
Figure 26: Illustration of the problem considering a static loading.

error constraint is set to $\beta = 0.05$, which means that only 5% of all design variables can change at each iteration. A filter radius of 6 grid sizes is chosen. The interpolation between materials is carried out using $p = 3$. The results obtained are presented below.

3.6.1.1 Structural mean compliance

In the first example, the goal is to minimize the structural mean compliance of the tower foundation. For comparison purposes, two cases are analyzed. In the first case, the optimization problem is solved considering the initial design domain completely full, i.e., filled with the stiffest material (foundation material). Since the design domain starts out full, the set of design variables of the initial TOBS optimization grid is described only by variables {1}. Then, we optimize the design with the initial domain filled only by the final volume fraction prescribed in the problem. Therefore, within the initial domain an area of dimension 4.0×4.05 m – i.e., 15% of material – is considered filled by solid foundation material. The convergence of the problem is evaluated by averaging the changes in the structural mean compliance (objective function) over 6 consecutive iterations for a tolerance of $\tau = 1 \cdot 10^{-5}$. Figure 32 presents the optimized structural layout for the two cases, the red region represents the foundation solid material (1) and the blue region corresponds to fictitious soil material (0).

The initial design domain has a big influence on the optimization process in most cases. In the scope of structural foundation designs, the layout to be obtained is very non-intuitive due to the different conditions present in this type of problem, in addition to the possible objectives to be achieved. As seen, different designs are obtained according to the assumed initial design domain. Figures 32(a) and (c) present the design reached considering the initial design domain full (filled entirely with foundation solid material). The optimized structure presents a semicircular shape with the presence of some holes inside the domain. In general, considering the initial domain
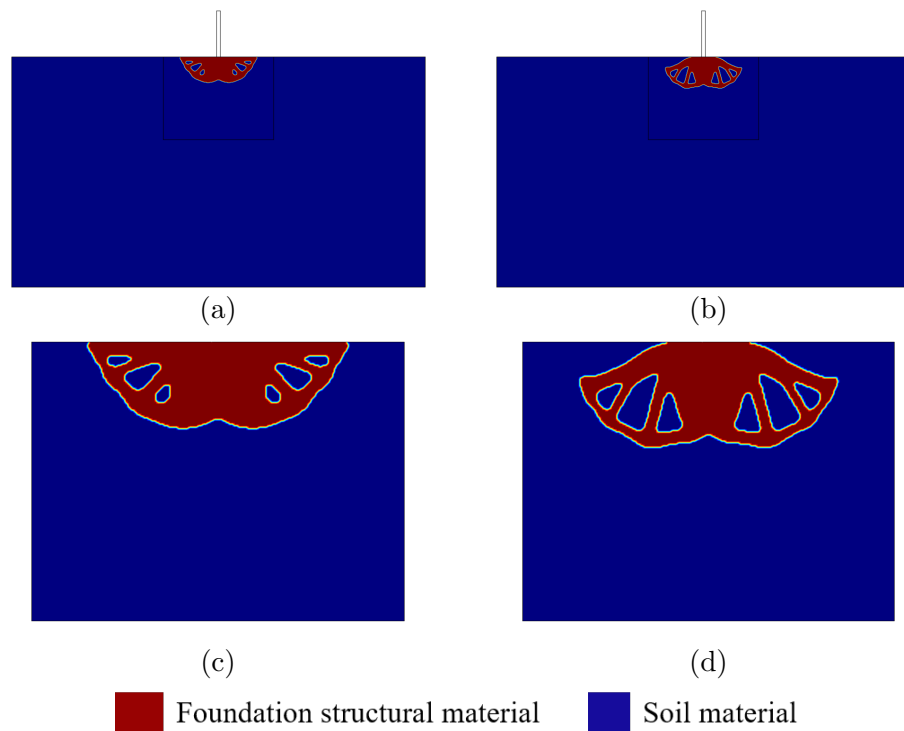
Figure 27: Structural foundation design optimized for minimum mean compliance: (a) optimized solution obtained starting with a full initial guess design and (b) optimized solution obtained starting with a volume fraction of 15%, (c) and (d) design domain of both cases, respectively. The red region corresponds to the domain of foundation solid material and the blue region to the soil material.

full allows a greater and better distribution of material, since the influence of each element is computed in the entire design domain and not just in a specific area. Figures 32(b) and (d) show the optimized layout for the second case, considering the initial design domain filled only with a fraction of the structural final volume. Unlike the first case, the optimized design has a distinct shape along with some thin bars in a truss-like shape within the structural domain. The evolution of the structural compliance (objective function) and volume fraction (constraint) along with some topology snapshots throughout the optimization is shown in Fig. 28 for both cases.

As it can be seen, the structural compliance presents a smooth convergence in both cases. In the first case – Fig. 28(a) –, a lower compliance value is observed at the beginning of the optimization once the initial design domain is filled entirely with the stiffest material. Throughout the entire optimization, the largest amount of foundation material is located in the upper part of the design domain, i.e., near the base of the tower structure. The structural foundation design is achieved in 147 iterations with a structural mean compliance value of 13.7001 Nm. In the second case, the structural compliance has a higher initial value due to the lower fraction of stiffer material within the design domain. It is possible to notice that there are no big changes in the topology after some iterations. Considering that the initial design domain is filled with the prescribed final volume fraction, the structural volume fraction remains the same during the whole optimization. The problem converges in 58 iterations to a structural compliance value of 14.3917 Nm. The optimized solution for this case is reached in a

smaller number of iterations since the constraint function (volume fraction) is satisfied since the beginning of the optimization. However, the global structural mean compliance value obtained is 5.05% higher than for the case considering the initial domain completely filled by structural material. The initial design domain is freely chosen when using the TOBS framework. Taking into account that each material is defined by a design variable, these being binary {0} or {1}, the optimization grid defined by the TOBS module allows the modeling of any initial geometry. In addition, topologies with well-defined contours are provided at all iterations.
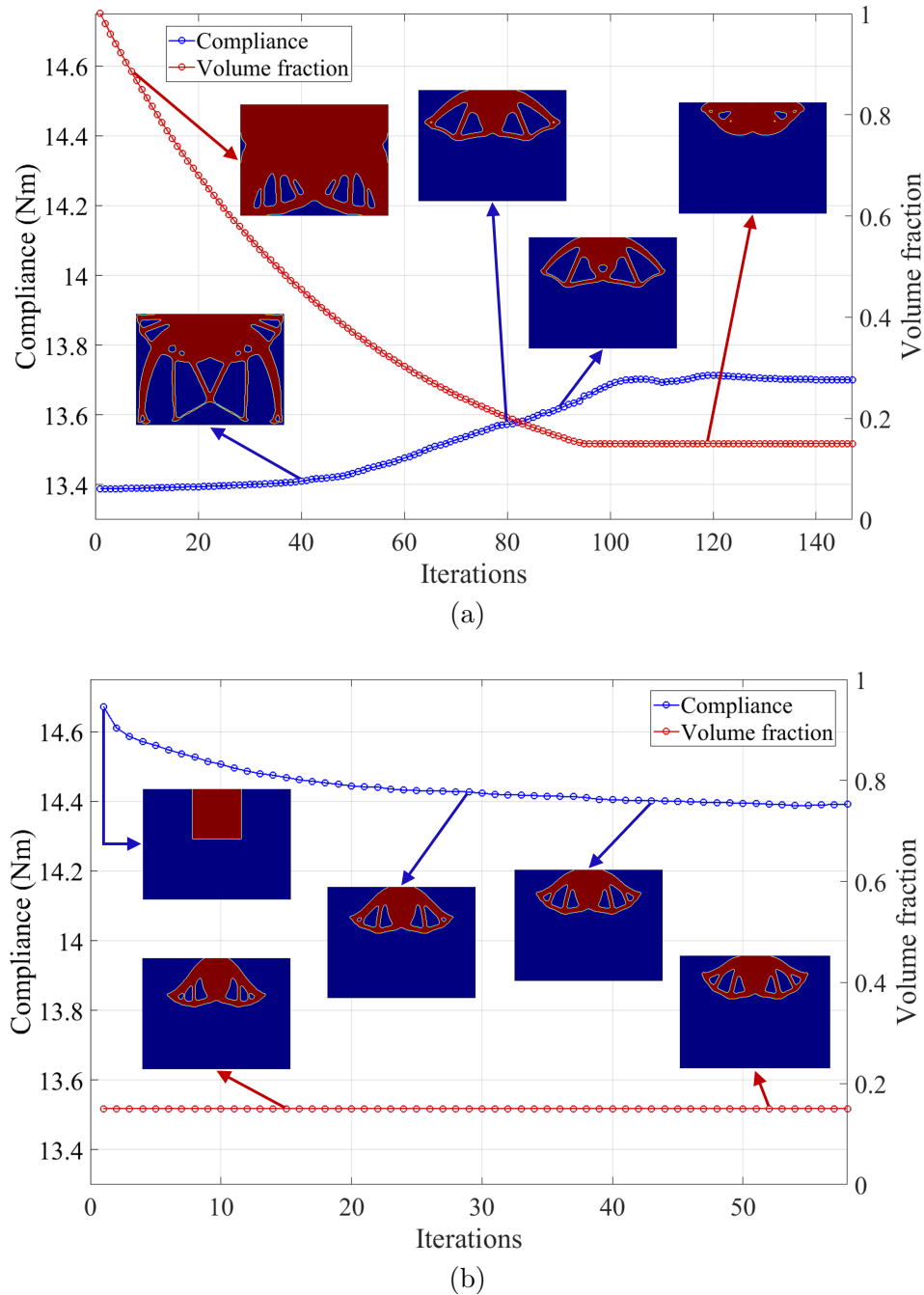

(a)

(b)

Figure 28: History of the structural compliance (objective function) and structural fraction volume (constraint function) along with topology snapshots throughout the optimization process for both cases: (a) initial design domain fully filled and (b) initial design domain partially filled.

3.6.1.2 Squared difference of the displacements

The objective of this example is to design the structural foundation topology in order to minimize the squared difference of the displacements between the points u_1 and u_2 (see Fig. 26). As in the previous example, two cases are solved. The topology is optimized by employing the initial design completely and partially filled with structural foundation material. The same area of dimension 4.0×4.05 m previously described is also considered in this example for the second case. The convergence criteria $\tau = 1 \cdot 10^{-4}$ is assigned to define the convergence of the problem. The optimized layouts obtained for both cases are shown in Fig. 29.

(a)   (b)

(c)   (d)

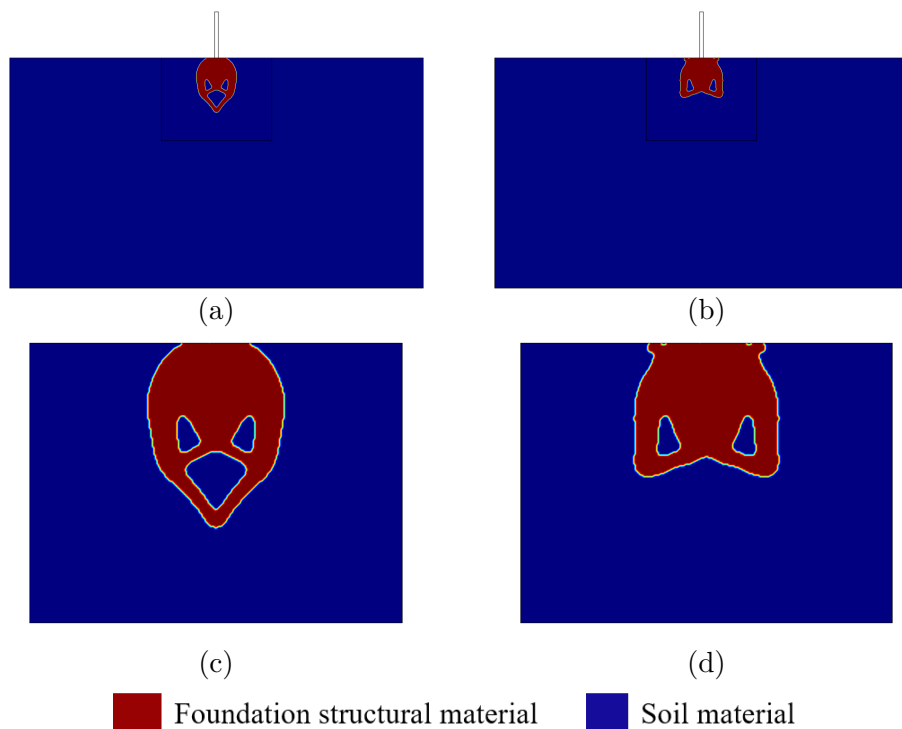■ Foundation structural material   ■ Soil material

Figure 29: Optimized structural foundation design for minimum squared difference of the displacements between two points: (a) and (b) optimized solution obtained starting with a full initial guess design and with a volume fraction of 15%, respectively, (c) and (d) design domain of both cases. The red color represents the structural foundation domain and the blue color the soil domain.

As it can be observed, the designs obtained show a significant difference between them. Figures 29(a) and 29(c) shows the optimized structural foundation design for the case employing the full initial domain (fully filled with foundation material). In this case, the underside of the optimized structure has a pointed contour and it is also possible to notice the presence of some holes filled with soil material within the domain. For the case of considering the initial domain only partially filled with foundation material – Figs. 29(b) and 29(d) – the pointed shape is not observed. However, it is still possible to notice the presence of some holes inside the structure filled with soil material. Figures 30(a) and 30(b) presents the convergence history of the objective and volume functions and some intermediate solutions throughout the optimization process for both cases. In the first case – Fig. 30(a) – the change from foundation material (1) to soil material (0) can be observed close to the boundaries of the design domain in the initial iterations. Over the optimization, the structure presents a certain elongation tendency below the

structural tower in addition to hook-shaped structures. The optimized solution is reached with a smooth convergence after 140 iterations with a squared difference of $7.2724 \cdot 10^{-4}$ m between the displacements of the two points. In the second case, the topology does not show major changes over the iterations. Since the constraint function is satisfied from the beginning of the optimization, the optimizer seeks the closest local minimum, thus, no big changes in the topology occur. In this case, the foundation structural design is obtained in 12 iterations with the squared difference of $7.2829 \cdot 10^{-4}$ m between the top and bottom points of the tower.
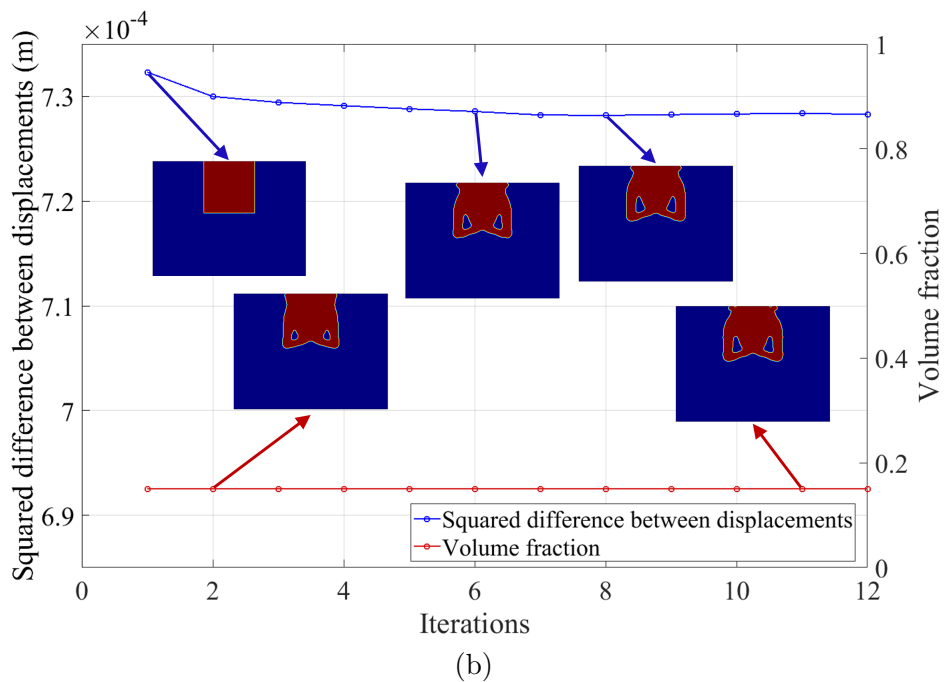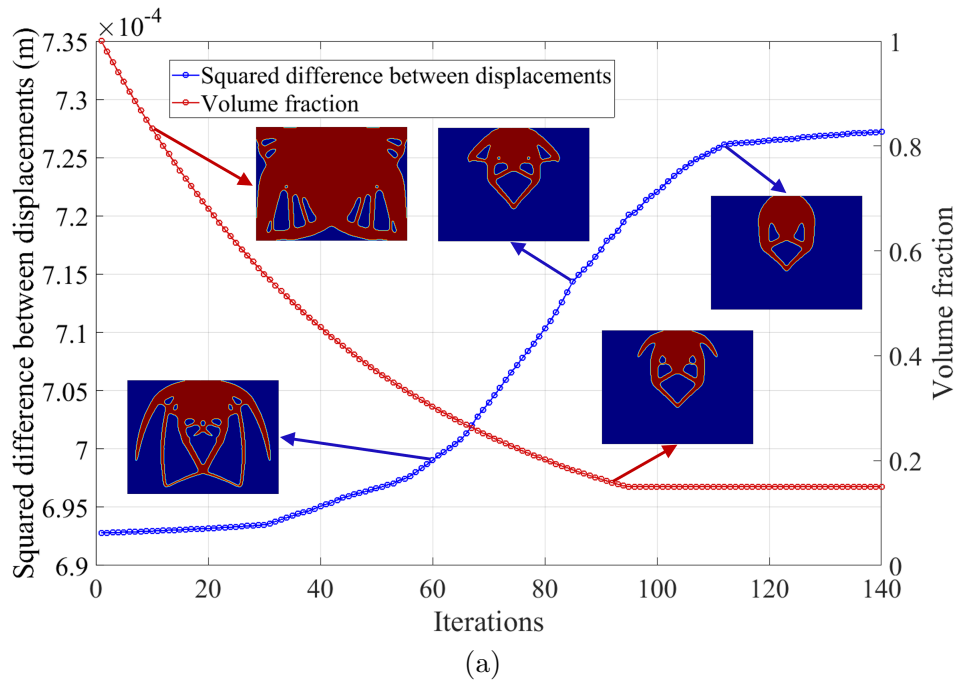

Figure 30: Convergence history of objective and constraint functions throughout the optimization along with intermediate solutions for both cases: (a) full initial guess design and (b) initial design domain partially filled with a volume fraction of 15%.

3.6.2 Dynamic case

Dynamic analysis in structural foundations design is of paramount importance since tower structures are subject to several phenomena where the inclusion of the dynamic regime is essential, such as earthquakes or ground movements due to events around the structure. In this example, the problem described in the previous example 3.6.1 is analyzed subject to a harmonic loading. For this, PML's are applied to the boundary of the soil domain in order to avoid wave reflection and, consequently, numerical problems. The representation of the problem is shown in Fig. 31. The objective is to find the structural foundation topology that minimizes the squared difference of displacements between the top and bottom points of the tower. The structural tower and foundation material is chosen to have Young's modulus $E = 2 \cdot 10^9$ Pa and density $\rho = 2500$ kg/m^3. The soil properties are Young's modulus $E = 21.5 \cdot 10^6$ Pa and density $\rho = 1250$ kg/m^3. An external horizontal load F $= 5 \cdot 10^4$ N is applied in the center of the soil domain P_1 (see Fig. 31). The point load is applied for the frequency $\omega = 1.8$ Hz. Convergence is defined by the average of the objective function changes over 6 consecutive iterations, with a tolerance of $1 \cdot 10^{-4}$ to stop the optimization.
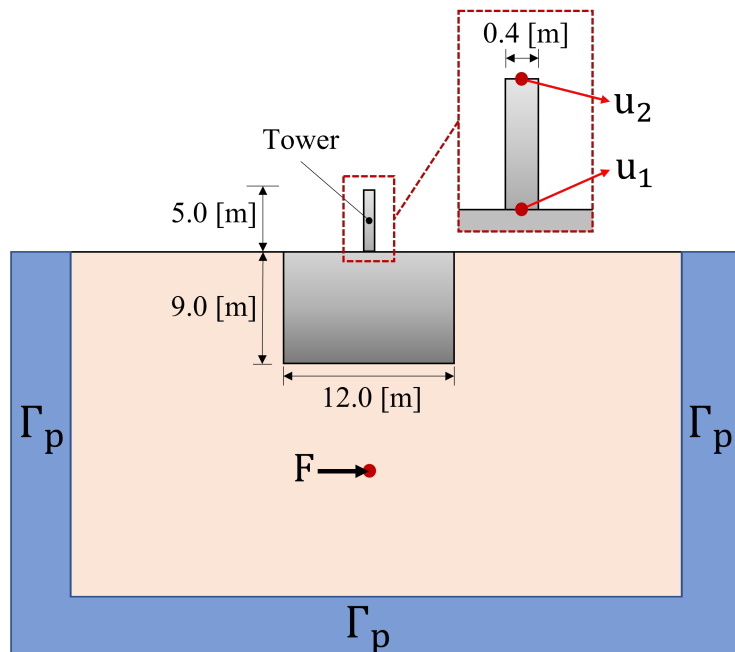
Figure 31: Illustration of the problem considering a dynamic loading.

The TOBS method is applied to design the structural foundation. The minimum squared difference between the displacements is solved subject to a volume fraction constraint with $\bar{V}$ = 15%. A filter radius of 6 is used. The constraint relaxation parameter is set as $\epsilon = 0.02$ and the truncation error constraint parameter is $\beta = 0.02$. The solid material penalization is $p = 3$. The optimized structural foundation layout is shown in Fig. 32.

In this case, it is noticed that the exchange of foundation elements for soil material elements starts at the upper corners of the structure. Figure 33 shows snapshots of the topology throughout the optimization process along with the constraint and objective function history. As in the previous cases, the boundaries between the two materials remains explicit throughout the entire optimization process. Some peaks are evident in the objective function due to the
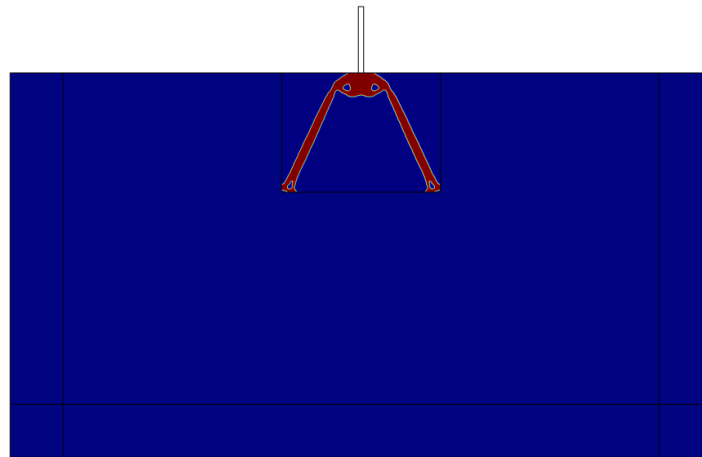
(a)
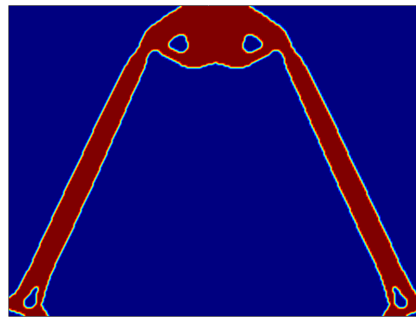
(b)

Foundation structural material   Soil material

Figure 32: Optimized solution of the structural foundation for minimum squared difference of the displacements between two points considering a dynamic loading: (a) optimized foundation design and (b) design domain. The red domain is the structural foundation and the blue one corresponds to the soil domain.

breaking of structural members which causes increased instability. The structural volume, which is regulated by the ϵ parameter, converges smoothly throughout the optimization until the prescribed volume fraction $\bar{V}$ and then remains constant until the convergence. The optimized solution is reached in 107 iterations and has a lower objective function value.
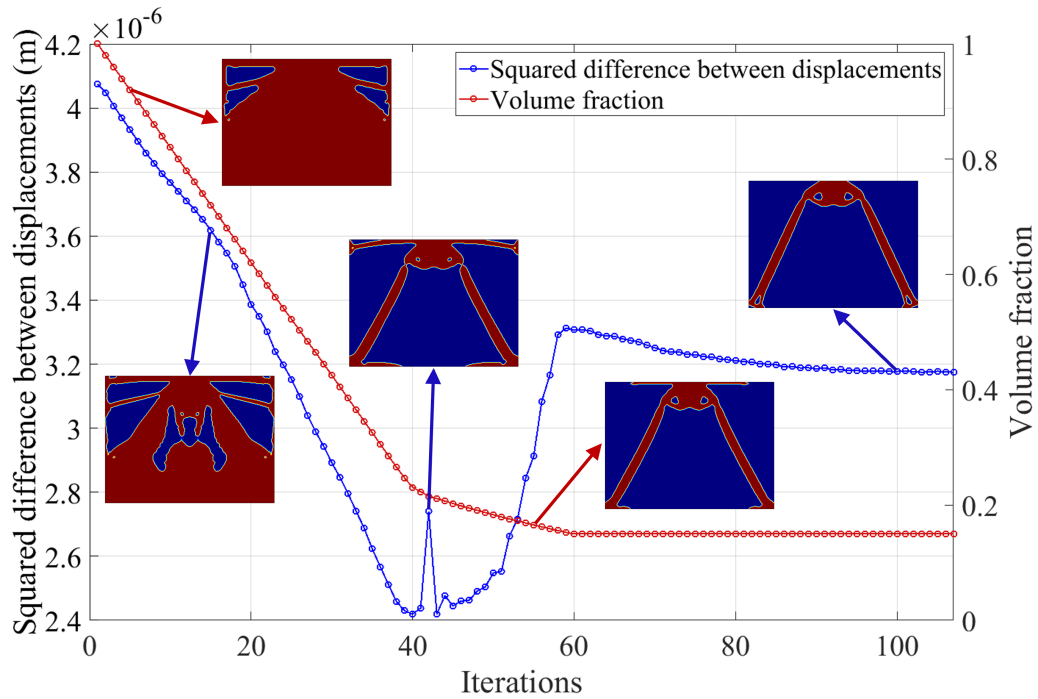
Figure 33: History of the objective function and the structural foundation volume (constraint) throughout the optimization process along with some topology snapshots.

3.7 Conclusions

This work developed a methodology to design structural foundations subject to static and dynamic loads. A large square region within the soil domain is defined as a design domain in order to design a foundation to support the structural tower above the ground. The optimization problem is performed by integrating the optimizer (TOBS) with an external FEA package. Two materials are considered in the optimization process: soil and structural foundation material. The material distribution is performed by the interpolation between the available materials. The TOBS method is employed to formulate and solve the optimization problem via integer linear programming. Decision variables indicate the material properties for each mesh element in the design domain, being either foundation material (variable 1) or soil (variable 0). The topology optimization problems considered include the minimization of the mean structural compliance and the minimization of the squared difference of the displacements between two specific points. Numerical examples shows that the proposed methodology can produce optimized designs with clear and explicit structural boundaries. Future works aims to extend the methodology to 3D structures and include more complex analysis, such as the consideration of geometric non-linearities and transient regimes.

4 CONCLUSIONS

The main contribution of this thesis is the development of topology optimization methodologies for tower-like structure designs involving fluid-structure interaction and soil-structure interaction. Herein, the two main components of this sort of mechanical system were addressed: the foundation and the structural tower. Both methodologies are based on structures with a clear definition of the structural boundary via the TOBS method, a binary approach. Presented in separate chapters, the research addressed two different types of topology optimization problems which present introduction, formulation and numerical application along with their respective discussions. The general conclusions about each optimization problem are presented below.

- Chapter 2 – *Topology optimization of stationary fluid-structure interaction problems including large displacements*: This topology optimization problem had as main objective to design stiff structures subject to viscous fluid loads considering large displacements. The main contribution to the optimization framework is the inclusion of nonlinear structural responses in the optimization of FSI systems. Furthermore, the decoupling of the module and the FEA is one of the advantages of the TOBS-GT method. The non-dependence between these two modules makes it feasible to apply the developed methodology to other multiphysics systems. In addition to the reasonably low computational cost due to the decrease in the total number of finite elements employed in the problem – the bottleneck of topology optimization – structures with clear structural boundaries are obtained. Moreover, an effective interface tracking is achieved throughout the entire optimization process – an important factor for problems involving more than one physics.

- Chapter 3 – *Structural foundation design via topology optimization and soil-structure interaction*: This topology optimization problem aimed to design foundation layouts for tower-like structures subjected to static and dynamic loads. The developed topology optimization framework allowed the consideration of more than one material in the optimization process, an advantageous feature for the design of structures in the geotechnical environment and multiphysics problems in general. In addition, structures closer to reality were obtained due to the consideration of dynamic loads and the use of binary variables, which provides accurate and clear designs in terms of structural boundaries.

4.1 Suggestions for future works

In general, the TOBS and TOBS-GT methods proved to be viable and presented satisfactory results in the design of problems involving fluid-structure interaction (FSI) and soil-structure interaction (SSI). The possibility of coupling and decoupling the analysis makes it possible to design structures with higher fidelity. We expect that the developed methodologies can contribute in the future to achieve new insights of tower-like structure designs considering FSI and SSI. Therefore, suggestions for future works are:

- To apply the developed methodologies to design wind towers in an integrative approach, i.e., optimizing the wind turbine as whole, coupling foundation and tower components.

- To include wall smoothing and high Reynolds numbers for the FSI system in order to obtain designs closer to reality, i.e., with higher airflow speed.

- To consider transient problems.

- To consider thermal expansion effects.

REFERENCES

[1] E Shreve. Wind turbine topples in south kent; 'extreme load of some kind' may have caused damage, says expert. `https://wind-watch.org/news/?p=86465`, 2018. National Wind Watch.

[2] S Fowler. Cracks in foundation led to wind turbine's collapse, 49 others also at risk. `https://www.cbc.ca/news/canada/new-brunswick/cracks-in-foundation-led-to-wind-turbine-collapse-1.6312668`, 2021. Canadian Broadcasting Corporation.

[3] A M Kaynia. Seismic considerations in design of offshore wind turbines. *Soil Dynamics and Earthquake Engineering*, 124:399–407, 2019.

[4] International Energy Agency (IEA). Wind electricity. `https://www.iea.org/reports/wind-electricity`, 2022.

[5] M Damgaard, V Zania, L V Andersen, and L B Ibsen. Effects of soil–structure interaction on real time dynamic response of offshore wind turbines on monopiles. *Engineering Structures*, 75:388–401, 2014.

[6] T S Sarpkaya. *Wave Forces on Offshore Structures*. Cambridge University Press, 2010.

[7] M Muskulus and S Schafhirt. Design optimization of wind turbine support structures-a review. *Journal of Ocean and Wind Energy*, 1:12–22, 02 2014.

[8] R Haghi, T Ashuri, P L C V D Valk, and D P Molenaar. Integrated multidisciplinary constrained optimization of offshore support structures. *Journal of Physics: Conference Series*, 555:012046, dec 2014.

[9] Energy Watch. Ørsted ceo says confidence not shaken by malfunction boom in danish offshore wind. `https://energywatch.com/EnergyNews/Renewables/article14304136.ece`, 2022.

[10] M P Bendsøe and O Sigmund. *Topology Optimization - Theory, Methods and Applications*. Springer Verlag, Berlin Heidelberg, 2003.

[11] K Patryniak, M Collu, and A Coraddu. Multidisciplinary design analysis and optimisation frameworks for floating offshore wind turbines: State of the art. *Ocean Engineering*, 251:111002, 2022.

[12] E H Dowell and K C Hall. Modeling of fluid-structure interaction. *Annual Review of Fluid Mechanics*, 33(1):445–490, 2001.

[13] Y Bazilevs, K Takizawa, and T E Tezduyar. *Computational Fluid-Structure Interaction: Methods and Applications*. Wiley, 2013.

[14] N Jenkins and K Maute. An immersed boundary approach for shape and topology optimization of stationary fluid-structure interaction problems. *Structural and Multidisciplinary Optimization*, 54:1191–1208, 2016.

[15] R Picelli, S Ranjbarzadeh, R Sivapuram, R S Gioria, and E C N Silva. Topology optimization of binary structures under design-dependent fluid-structure interaction loads. *Structural and Multidisciplinary Optimization*, 62:2101–2116, 2020.

[16] J Alexandersen and C S Andreasen. A review of topology optimisation for fluid-based problems. *Fluids*, 5(1), 2020.

[17] M I Blanco. The economics of wind energy. *Renewable and Sustainable Energy Reviews*, 13(6-7):1372–1382, August 2009.

[18] R Sivapuram and R Picelli. Topology optimization of binary structures using integer linear programming. *Finite Elements in Analysis and Design*, 139:49–61, 2018.

[19] E Mendes, R Sivapuram, R Rodriguez, M Sampaio, and R Picelli. Topology optimization for stability problems of submerged structures using the tobs method. *Computers Structures*, 259:106685, 2022.

[20] K E S Silva, R Sivapuram, S Ranjbarzadeh, E S Gioria, E C N Silva, and R Picelli. Topology optimization of stationary fluid–structure interaction problems including large displacements via the tobs-gt method. *Structural and Multidisciplinary Optimization*, 65:337, 2022.

[21] F Casadei, J P Halleux, A Sala, and F Chillè. Transient fluid–structure interaction algorithms for large industrial applications. *Computer Methods in Applied Mechanics and Engineering*, 190(24):3081–3110, 2001. Advances in Computational Methods for Fluid-Structure Interaction.

[22] G P Galdi and R Rannacher. *Fundamental Trends in Fluid-structure Interaction*. Contemporary challenges in mathematical fluid dynamics and its applications. World Scientific, 2010.

[23] T Bodnár, G Galdi, and S Nečasová. *Fluid-Structure Interaction and Biomedical Applications*. 01 2014.

[24] R Kamakoti and W Shyy. Fluid–structure interaction for aeroelastic applications. *Progress in Aerospace Sciences*, 40(8):535–558, 2004.

[25] M P Païdoussis. *Fluid-structure interactions: Slender structures and axial flow*, volume 1. Academic Press, 1998.

[26] C S Andreasen and O Sigmund. Topology optimization of fluid-structure interaction problems in poroelasticity. *Computer Methods in Applied Mechanics and Engineering*, 258:55–62, 2013.

[27] W M Vicente, R Picelli, R Pavanello, and Y M Xie. Topology optimization of frequency responses of fluid-structure interaction systems. *Finite Elements in Analysis and Design*, 98:1–13, 2015.

[28] J Kook and J S Jensen. Topology optimization of periodic microstructures for enhanced loss factor using acoustic–structure interaction. *International Journal of Solids and Structures*, 122-123:59–68, 2017.

[29] J Zhu, H Zhou, C Wang, L Zhou, S Yuan, and W Zhang. A review of topology optimization for additive manufacturing: Status and challenges. *Chinese Journal of Aeronautics*, 34(1):91–110, 2021.

[30] H J Bungartz and M Schäfer. *Fluid-structure Interaction: Modelling, Simulation, Optimization.* Berlin Heidelberg, 2006.

[31] A E Hami and B Radi. *Fluid-Structure Interactions and Uncertainties: Ansys and Fluent Tools*. Mechanical Engineering and Solid Mechanics: Reliability of Multiphysical Systems. Wiley, 2017.

[32] T Richter. *Fluid-structure Interactions: Models, Analysis and Finite Elements.* Lecture Notes in Computational Science and Engineering. Springer International Publishing, 2017.

[33] C Lundgaard, J Alexandersen, M Zhou, C Andreasen, and O Sigmund. Revisiting density-based topology optimization for fluid-structure-interaction problems. *Structural and Multidisciplinary Optimization*, 58:969–995, 2018.

[34] K Maute and M Allen. Conceptual design of aeroelastic structures by topology optimization. *Structural and Multidisciplinary Optimization*, 27(1–2):27–42, 2004.

[35] N Jenkins and K Maute. Level set topology optimization of stationary fluid-structure interaction problems. *Structural and Multidisciplinary Optimization*, 52(1):179–195, 2015.

[36] G H Yoon. Topology optimization for stationary fluid-structure interaction problems using a new monolithic formulation. *International Journal for Numerical Methods In Engineering*, 82:591–616, 2010.

[37] G H Yoon. Stress-based topology optimization method for steady-state fluid-structure interaction problems. *Computer Methods in Applied Mechanics and Engineering*, 278:499–523, 2014.

[38] R Picelli, A Neofytou, and H A Kim. Topology optimization for design-dependent hydrostatic pressure loading via the level-set method. *Structural and Multidisciplinary Optimization*, 60:1313–1326, 2019.

[39] F Feppon, G Allaire, C Dapogny, and P Jolivet. Topology optimization of thermal fluid–structure systems using body-fitted meshes and parallel computing. *Journal of Computational Physics*, 417:109574, 2020.

[40] H Li, T Kondoh, P Jolivet, K Furuta, T Yamada, B Zhu, K Izui, and S Nishiwaki. Three-dimensional topology optimization of a fluid–structure system using body-fitted mesh adaption based on the level-set method. *Applied Mathematical Modelling*, 101:276–308, 2021.

[41] R Sivapuram and R Picelli. Topology design of binary structures subjected to design-dependent thermal expansion and fluid pressure loads. *Structural and Multidisciplinary Optimization*, 61:1877–1895, 2020.

[42] R Picelli, W M Vicente, and R Pavanello. Evolutionary topology optimization for structural compliance minimization considering design-dependent FSI loads. *Finite Elements in Analysis and Design*, 135:44–55, 2017.

[43] X Huang and Y M Xie. Convergent and mesh-independent solutions for the bi-directional evolutionary structural optimization method. *Finite Elements in Analysis and Design*, 43:1039–1049, 2007.

[44] R Picelli, E Moscatelli, P Yamabe, D Alonso, S Ranjbarzadeh, R Gioria, J Meneghini, and E C N Silva. Topology optimization of turbulent fluid flow via the tobs method and a geometry trimming procedure. *Structural and Multidisciplinary Optimization*, 65, 01 2022.

[45] R Picelli, R Sivapuram, and Y M Xie. A 101-line MATLAB code for topology optimization using binary variables and integer programming. *Structural and Multidisciplinary Optimization*, 63:935–954, 2020.

[46] P M Gresho and R L Sani. *Incompressible Flow and the Finite Element Method*. Wiley, 2000.

[47] P Wriggers. *Nonlinear Finite Element Methods*. Springer Berlin Heidelberg, 2008.

[48] B Gatzhammer. *Efficient and Flexible Partitioned Simulation of Fluid-Structure Interactions*. PhD thesis, Technical University of Munich, Germany, 2014.

[49] E Lund, H Møller, and L Jakobsen. Shape design optimisation of stationary fluid-structure interaction problems with large displacement and turbulence. *Structural and Multidisciplinary Optimization*, 25:383–392, 01 2003.

[50] A H Land and A G Doig. An automatic method of solving discrete programming problems. *Econometrica*, 28:497–520, 1960.

[51] R T Haftka and Z Gürdal. *Elements of Structural Optimization*. Kluwer Academic Publishers, 3rd rev. and expanded ed. edition, 1991.

[52] R Picelli, W M Vicente, and R Pavanello. Bi-directional evolutionary structural optimization for design-dependent fluid pressure loading problems. *Engineering Optimization*, 47(10):1324–1342, 2015.

[53] W G Curtin, G Shaw, G G Parkinson, J Golding, and N Seward. *Structural Foundation Designers' Manual*. Wiley, 2008.

[54] D P Coduto. *Foundation Design: Principles and Practices*. Prentice Hall, 1994.

[55] J Wu, O Sigmund, and J P Groen. Topology optimization of multi-scale structures: A review. 63(3), 2021.

[56] Z Huang and S Hinduja. Shape optimization of a foundation for a large machine tool. *International Journal of Machine Tool Design and Research*, 26(2):85–97, 1986.

[57] Z Sienkiewicz and B Wilczyński. Shape optimization of a dynamically loaded machine foundation coupled to a semi-infinite inelastic medium. *Structural Optimization*, 12:29–34, 1996.

[58] T William Lambe and Robert V Whitman. *Soil mechanics*, volume 10. John Wiley & Sons, 1991.

[59] C H Juang and L Wang. Reliability-based robust geotechnical design of spread foundations using multi-objective genetic algorithm. *Computers and Geotechnics*, 48:96–106, 2013.

[60] L Hui, C Zhuoyi, and Z Mingji. Genetic algorithm application on optimal design of strip foundation. *The Open Cybernetics Systemics Journal*, 9:335–339, 05 2015.

[61] J H Holland. *Adaptation in Natural and Artificial Systems.* University of Michigan Press, 1975.

[62] J H Holland. *Adaptation in natural and artificial systems: an introductory analysis with applications to biology, control, and artificial intelligence.* MIT press, 1992.

[63] J Grabe and T Pucker. Beitrag zum entwurf und zur ausführung von kombinierten pfahl-plattengründungen. *Bautechnik*, 88(12):828–835, 2011.

[64] K Seitz and J Grabe. Topology optimization for the design of structures. 09 2015.

[65] K Seitz and J Grabe. Three-dimensional topology optimization for geotechnical foundations in granular soil. *Computers and Geotechnics*, 80:41–48, 2016.

[66] K Zied, F Mohamed, and S Hichem. Direct limit analysis based topology optimization of foundations. *Soils and Foundations*, 59(4):1063–1072, 2019.

[67] R Sivapuram, R Picelli, G H Yoon, and B Yi. On the design of multimaterial structural topologies using integer programming. *Computer Methods in Applied Mechanics and Engineering*, 384:114000, 2021.

[68] S Sadeghi, F Abedini, R D Reza, and L Karim. Covariance matrix adaptation evolution strategy for topology optimization of foundations under static and dynamic loadings. *Computers and Geotechnics*, 140:104461, 2021.